Journal of Sound and Vibration 634 (2026) 119739

Contents lists available at ScienceDirect

Journal of Sound and Vibration

journal homepage: www.elsevier.com/locate/jsvi

Aeroacoustics research in Europe: The CEAS-ASC report on 2024 highlights

Luminiţa Drăgăşanu [a,*], Damiano Casalino [b], Narcisa Burtea [a]

[a] COMOTI - Romanian Research and Development Institute for Gas Turbines, Iuliu Maniu 220D, Bucharest, 061126, Romania
[b] Flow Physics and Technology Department, Kluyverweg 1, Delft, 2629 HS, The Netherlands

ARTICLE INFO

Keywords:
Aeroacoustics
Airframe noise
Propeller noise
Acoustic liners meta-materials
Experimental techniques
Urban air mobility noise

ABSTRACT

The report presents a curated overview of the most relevant research activities in Aeroacoustics conducted across Europe during 2024. Compiled by the Aeroacoustics Specialists' Committee (ASC) of the Council of European Aerospace Societies (CEAS), the contributions span multiple topical areas, including airframe noise, propeller noise, acoustic liners and metamaterials, experimental methodologies, and noise associated with urban air mobility platforms. Notable advancements are summarised in each section, many of which stem from nationally or internationally funded collaborative projects. In addition, this edition includes highlights from major Aeroacoustic events such as the 25th CEAS-ASC Workshop held in Bucharest and the 30th AIAA/CEAS Aeroacoustics Conference and Anniversary Ceremony in Rome. The purpose of the document is to support knowledge exchange within the European Aeroacoustic community and provide a reference point for current and emerging research directions. Enquiries concerning all contributions should be addressed to the authors whose contact information is provided at the end of each subsection.

1. Introduction

The Aeroacoustics Specialist's Committee of CEAS annually compiles an overview of recent research and development activities in the field of aeroacoustics across Europe. This report presents highlights from 2024, reflecting the most significant scientific and technological advancements as contributed by experts in the community.

Aeroacoustics, in its broadest sense, encompasses the study and control of noise generation and propagation in aerospace systems – from conventional aircraft engines and airframes to emerging propulsion concepts and Urban Air Mobility (UAM) platforms. The contributions gathered in this edition are grouped by thematic areas, including airframe noise, propeller noise, fan and jet noise, acoustic liners and metamaterials, experimental techniques, and noise in UAM configurations.

Many of the reported results are outcomes of collaborative efforts under nationally or internationally funded projects, and they represent peer-reviewed work published in 2024. In addition to scientific contributions, this report also includes brief accounts of relevant conferences and events held during the year, such as the 25th CEAS-ASC Workshop in Bucharest and the 30th AIAA/CEAS Aeroacoustics Conference and Anniversary Ceremony in Rome.

The present paper aims to provide the aeroacoustics community with a concise but comprehensive overview of ongoing developments in the field, supporting knowledge exchange and encouraging future collaborations.

* Corresponding author.
E-mail addresses: luminta.dragasanu@comoti.ro (L. Drăgăşanu), d.casalino@tudelft.nl (D. Casalino), narcisa.burtea@comoti.ro (N. Burtea).

https://doi.org/10.1016/j.jsv.2026.119739
Received 30 October 2025; Received in revised form 11 February 2026; Accepted 2 March 2026
Available online 5 March 2026

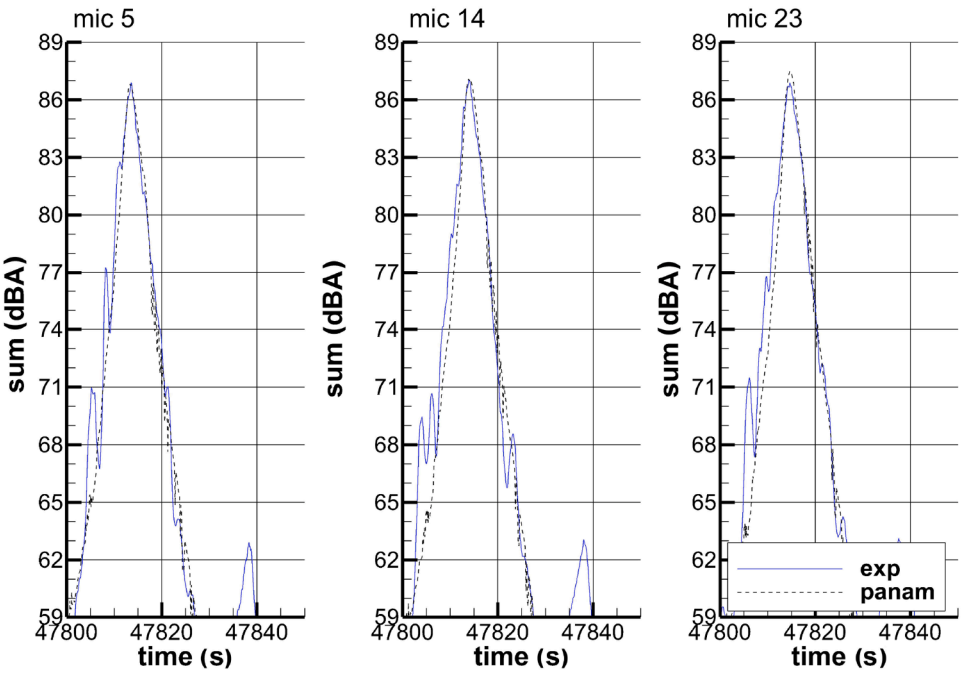

Fig. 1. Assessment of noise mitigation measures: Measured (blue) vs. PANAM results (black). (For interpretation of the references to colour in this figure legend, the reader is referred to the web version of this article.)

2. Airframe noise

2.1. Retrofit measures for aircraft noise reduction: Simulation benchmark and impact assessment

Retrofit measures to mitigate aircraft noise for conventional mid-range transportation aircraft have been under investigation at the German Aerospace Center (DLR) for many years. In 2016, the Advanced Technology Research Aircraft (ATRA) DLR testbed was subject to a dedicated flight campaign to evaluate the noise for the original vehicle without additional measures. Selected measures from previous research activities over the last years, i.e., with the main focus on airframe noise reduction, have then been installed on board and evaluated in a follow-on campaign under similar test conditions and settings in 2019. Based on recorded flight data and noise levels during both flight campaigns, a detailed evaluation was enabled for the first time to quantify the impact of these retrofit measures if operated on board of a real aircraft.[1]

Based on the 2016 and 2019 flight tests, a simulation activity was enabled that is presented in Bertsch et al. [1]. From the extensive amount of collected data a simulation model was derived and implemented into DLR's system noise prediction tool PANAM (Parametric Aircraft Noise Analysis Module). With this model, the noise impact of the ATRA with and without retrofit measures can be fully modelled along arbitrary flights.

In Bertsch et al. [1], the noise mitigation potential measured in the 2019 campaign can be confirmed by the simulation. It is demonstrated, that all of the recorded noise measurements from both flight campaigns could be reproduced with a very close agreement between measurement and simulation. The ATRA in its original configuration is predicted with a standard deviation of 0.81 dBA on the maximum A-weighted sound pressure level (LAmax). If the retrofit measures are applied, this standard deviation of the predicted LAmax increases slightly to 0.96 dBA. The overall allignment of simulation and experiment is depicted for an arbitrary observer location in Fig. 1. More details and statistics are provided in Bertsch et al. [1]. Based on these comparisons it can be concluded, that the effect of the retrofit measures is captured by the simulation and a full-blown system noise assessment of the ATRA with and without retrofit measures is enabled.

The retrofit measures are now assessed along typical approach procedures with their complex orchestra of noise sources on board that varies with operating condition. The overall effect of the retrofit measures on ground noise contours, i.e., LAmax and Sound Exposure Level (SEL), can now be assessed. A maximum noise reduction up to 5 dBA is predicted for certain regions along the approach with dominating airframe noise contribution. These results confirm the initially assumed significant mitigation potential for the proposed retrofit measures. The significant effect of the measures on the instantaneous contours of the LAmax are depicted in Fig. 2.

[1] Details for both campaigns is provided in previous publications that are listed in Bertsch et al. [1].

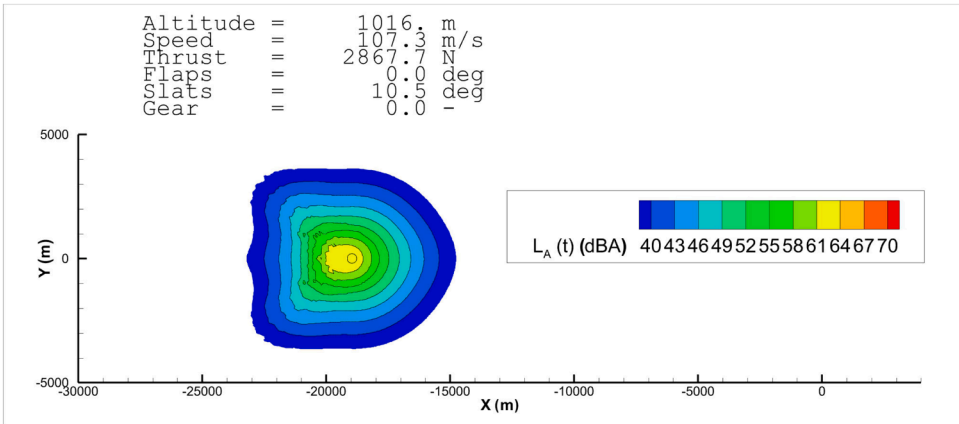

Fig. 2. Instantaneous impact of mitigation measure along approach procedure.

Written by Lothar Bertsch: lothar.bertsch@dlr.de, Michael Pott-Polenske, Felix Wienke, Joscha Kurz, and Jan Delfs, German Aerospace Center (DLR), Germany

2.2. Relevance of quadrupole diffraction on flow-induced noise from porous-coated cylinders

Coating a cylinder with a porous material represents an effective passive strategy to reduce the aerodynamic noise associated with vortex shedding. Despite numerous studies conducted in recent decades, the sound attenuation mechanisms associated with this technology remain unclear. Zamponi et al. [2] elucidated the link between the near-wake development of a porous circular cylinder and the measured aerodynamic sound attenuation by combining sound source localisation and flow visualisation techniques and formulating the related flow-induced noise as a diffraction problem.

The experimental findings showed that porosity causes a significant downstream displacement of dominant sound sources, which are not located on the cylinder surface but rather in the wake, at the onset of vortex-shedding instability, where the turbulence kinetic energy peaks (see Fig. 3). The analytical results revealed that, at the vortex-shedding frequency, aerodynamic noise can be effectively modeled as being generated by a compact lateral quadrupole radiating from the shedding-instability onset location and scattering into the far field with a quasi-dipolar directivity due to its diffraction by the body (see Fig. 3). This sound generation mechanism, which could not be derived using a classical approach based on Curle's analogy where volume terms are neglected, was successfully validated against measurements using a Green's function tailored to a cylindrical geometry.

The study demonstrated that the porous coating has a two-fold effect: it weakens the quadrupole in the wake and, more significantly, shifts its origin further downstream, thereby reducing the effectiveness of sound scattering. As a result, the diffracted component of the acoustic field, which, according to classical theory, dominates the far-field noise for a bare cylinder, becomes comparable in amplitude to the direct component, even at low Mach numbers.

Written by Riccardo Zamponi: r.zamponi@tudelft.nl, Technische Universiteit Delft, The Netherlands

3. Propeller noise

3.1. Phase cancelation of interaction noise for counter-rotating propellers

Counter-Rotating Propellers (CRPs) have garnered renewed interest in recent decades, primarily due to their high fuel efficiency. However, the more pronounced sound emission limits its use in civil aviation. This study investigates the interaction noise generated by CRPs [3], focusing on the role of surface pressure fluctuations in interaction noise generation. To this end, Lattice Boltzmann Method simulations are employed with the Ffowcs-Williams and Hawkings (FWH) analogy.

A new noise localisation method using Dynamic Mode Decomposition was introduced to map noise source distribution over the propeller blades and explore noise reduction mechanisms via phase cancellation. Compared to standard beamforming, this method provides greater insight by identifying noise contributions at specific frequencies and observer locations, depicted in the top view of Fig. 4(a). Surface noise analysis reveals that interaction tone noise is predominantly concentrated along the leading edge of the rear blade. Noise cancellation is achieved by controlling the distribution of positive and negative noise sources on the suction surface of the rear blade. This cancellation effect is closely linked to the relative positioning of the front blade's wake and the rear blade elements. By adjusting the rear blade sweep as seen in bottom view of Fig. 4(a), thereby modifying the aforementioned relative position, interaction noise can be effectively reduced.

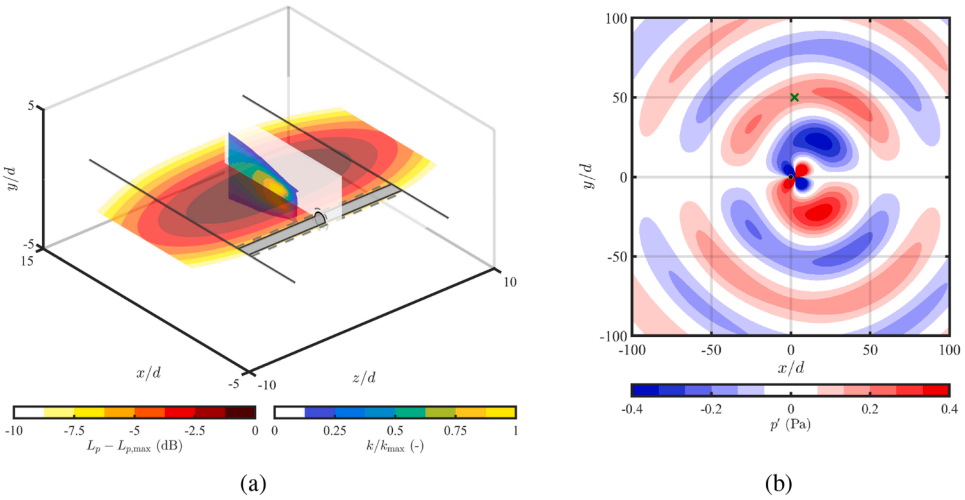

Fig. 3. (a) the acoustic sound map of a porous coated cylinder for a one-third octave frequency band of 2.5 kHz superimposed on the turbulence kinetic energy contour. The maps are normalised by their respective maximum values. (b) a snapshot of the total acoustic pressure radiated at the vortex-shedding frequency.

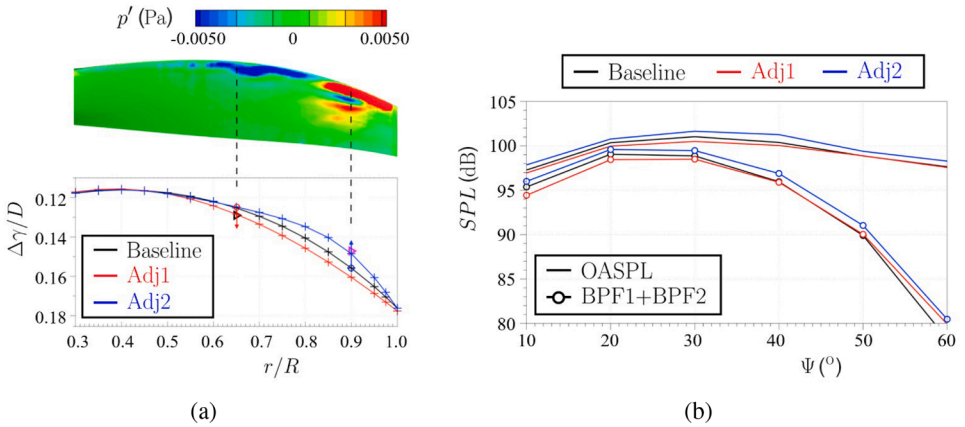

Fig. 4. (a) Surface pressure p' contribution (of baseline configuration) to the first interaction tone BPF1 + BPF2, and adjustment of rear blade sweep. (b) Upstream directivity of rear blade noise due to (aft) blade sweep adjustments.

The primary factor influencing interaction tone noise is the derivative of unsteady pressure fluctuations, which is strongly correlated with the radial vorticity of the front blade's wake. Optimising blade sweep configurations minimises the negative surface pressure region, leading to a significant reduction in interaction noise, as seen in Fig. 4(b).

The study demonstrates that modifying the rear blade sweep not only substantially reduces noise during take-off but also maintains propulsive performance across both take-off and cruise phases. These findings suggest that blade-sweep adjustments offer a promising approach to mitigating CRP noise, enhancing their feasibility for civil aviation applications.

Written by Rinie Akkermans: rinie.akkermans@haw-hamburg.de, Hamburg University of Applied Sciences, Germany, Tianxiang Hu, Beihang University, China and Changhao Lyu, TU Braunschweig, Germany.

3.2. Aerodynamics and aeroacoustics of propeller in non-conventional conditions

Electric-powered propellers have the advantage that they can be operated and installed in non-conventional ways. For example, they can be installed in co-rotating configurations [4], or operated at negative thrust [5,6]. For both configurations, high-fidelity numerical simulations were performed, identifying key fluid-dynamics aspects affecting far-field noise.

Two co-rotating 2×2 propellers, at a fixed axial distance, and two azimuthal spacings were investigated for the former case [4]. Results have shown that far-field noise can be reduced by promoting destructive interference. However, when the azimuthal angle spacing is small, potential aerodynamic effects dominate, reducing the aerodynamic potential benefit of co-rotating propellers. Therefore, aerodynamic optimisation is required, e.g., by changing the pitch angle between the two axially-spaced propellers.

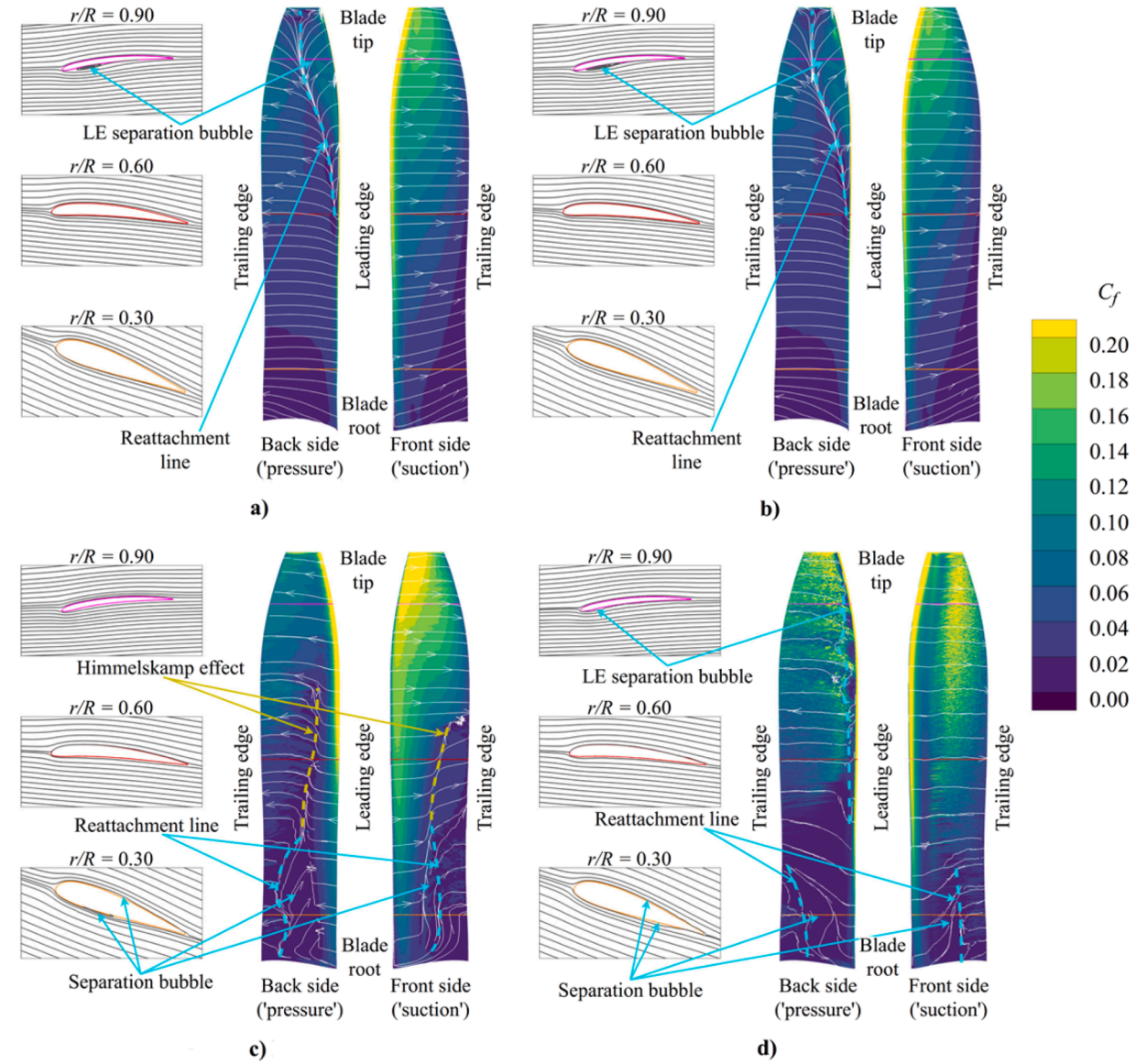

Fig. 5. Visualisation of flow around propeller blades at the positive thrust condition (J = 0.60) using skin friction coefficient and shear lines: a) SRANS, b) URANS, c) LB-VLE$_{y^+\geq 15}$, d) LB-VLES$_{y^+\leq 10}$.

Propellers operating at negative thrust settings [5,6] have the potential to reduce landing run, community noise, and provide energy regeneration. Numerical methods with increasing levels of fidelity, i.e., Blade Element Momentum Theory (BEMT), Reynolds-Averaged Navier-Stokes (RANS), Unsteady Reynolds-Averaged Navier-Stokes (URANS) and Lattice Boltzmann Method combined with Very Large Eddy Simulation (LBM-VLES), were compared and benchmarked against experimental data, highlighting the challenges and needs of wall-resolved numerical simulations and wake refinement to capture the dominant flow features, such as flow separation Fig. 5. In the negative thrust setting, the amplitude of the blade loading fluctuations is up to 18% for inboard sections and 30% near the blade tip compared to the time-averaged loads. This causes an increase in broadband noise, up to 15 dB along the propeller axis, but a reduction up to 10 dB in the propeller plane for a given absolute value of thrust coefficient [6].

Written by Francesco Avallone: francesco.avallone@polito.it, Politecnico di Torino, Italy

3.3. Low-reynolds number rotor noise

Small unmanned aerial vehicles (UAV) are now used in a wide range of applications, raising the question of public acceptance associated, in part, with noise emission. To investigate the noise generated by isolated small-scale UAV rotors operating under hovering

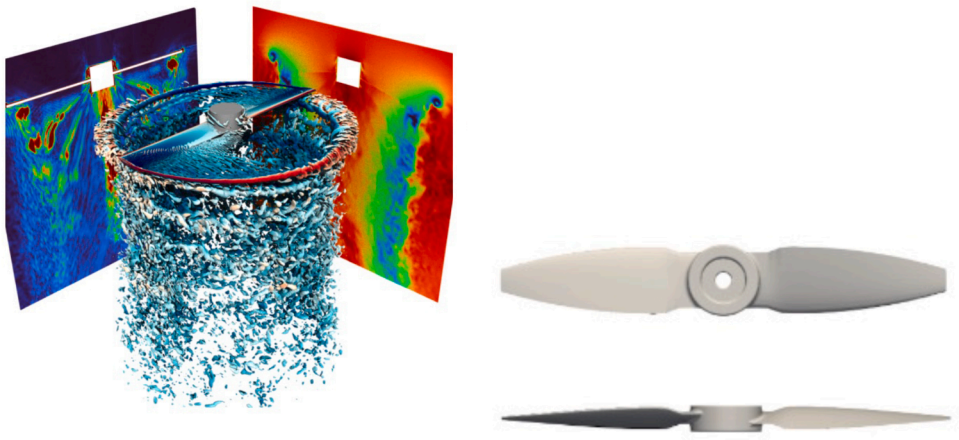

(a) (b)

Fig. 6. (a) Instantaneous Q-criterion isosurfaces coloured by vertical velocity and contours of instantaneous vorticity and velocity magnitudes; and (b) optimised geometry.

conditions, an open experimental database, accessible to the community, was created.[2] It may serve as a benchmark for the assessment of numerical approaches. The rotors have simplified geometries with NACA0012 profiles extruded in the radial direction with constant pitch and chord length. Those rotors are characterised by tonal noise at the blade passing frequency (BPF) and harmonics, a pronounced broadband noise, and flow separation. Accurate numerical prediction of the latter topology is challenging.

From this experimental set-up, Large Eddy Simulation (LES) relying on the massively parallel solver IC3 solving the compressible Navier-Stokes equations [7] (NS) were performed. The simulation (Fig. 6-a) captured well the boundary layer transition, the mean aerodynamic coefficients, and the tonal noise, but struggled to accurately reproduce the broadband trailing edge noise, stressing that accurate numerical prediction of the flow topology in such a transitional regime is still a challenge.

Since the previous rotors were not fully representative of realistic shapes, an optimisation of the chord and twist distributions was achieved to enhance both aerodynamic efficiency and noise reduction at the blade passing frequency. The resulting Pareto front produced three optimal shapes that were 3-D printed and experimentally tested to validate the optimisation process [8]. The most aerodynamically efficient geometry is presented in Fig. 6-b.

Written by Romain Gojon: romain.gojon@isae-supaero.fr, ISAE-SUPAERO, France

3.4. Multi-disciplinary optimisation of propeller blades

A multi-disciplinary design optimisation framework is presented to improve the aerodynamic performance and noise emission for quadcopters in forward flight by modifying the blade chord and sweep angle [9]. Unsteady RANS equations are solved using a commercial solver (STAR-CCM+) to evaluate unsteady blade loading. An in-house aeroacoustic solver, BATMAN$^{\pi}$, developed at the Von Karman Institute for Fluid Dynamics, is employed for the resulting acoustic radiation. The optimisation uses a Kriging-based surrogate model to minimise the Sound Power Level (SWL) at the blade passing frequency harmonics (BPFHs).

Aerodynamic assessment showed strong tip-on-tip and tip-on-strut interactions causing thrust fluctuations in forward flight, which affect tonal emissions at the blade loading harmonics (BLHs) up to order 10. Two optimisation cases are presented. In the first case, the 1st BPFH is minimised while keeping the time-averaged thrust value greater than 90% of the baseline. The SWL is decreased by approximately 1 dB. The optimiser cannot reduce the SWL further at 1st BPFH due to its tight link with 0th-order BLH, which is correlated with mean thrust. This showed that steady loading itself, indeed, plays a significant role in noise generation which makes it practically impossible to reduce the generated noise by only changing blade sweep and chord distributions.

In the second case, the spectrum is A-weighted and the 3rd BPFH (now the loudest, as depicted in Fig. 7) is selected as the objective function to better reflect human perception. Here, the SWL amplitude is predominantly influenced by unsteady blade loading, yielding a reduction of about 3.5 dB at the 3rd BPFH while also having appreciable reductions at other harmonics with the new sweep angle of approximately 40 deg (see Fig. 7).

The work showed the capabilities of a novel constrained optimisation framework for the blades of a quadcopter in forward flight. A significant noise reduction (3.5 dB) is achieved with a moderate reduction in propeller thrust (about 8%), which highlight the effectiveness of the URANS based computational fluid dynamics (CFD) solver coupled with the in-house aeroacoustic solver in a multidisciplinary framework as well as the efficiency of the surrogate model.

[2] doi.org/10.34849/C73YB7

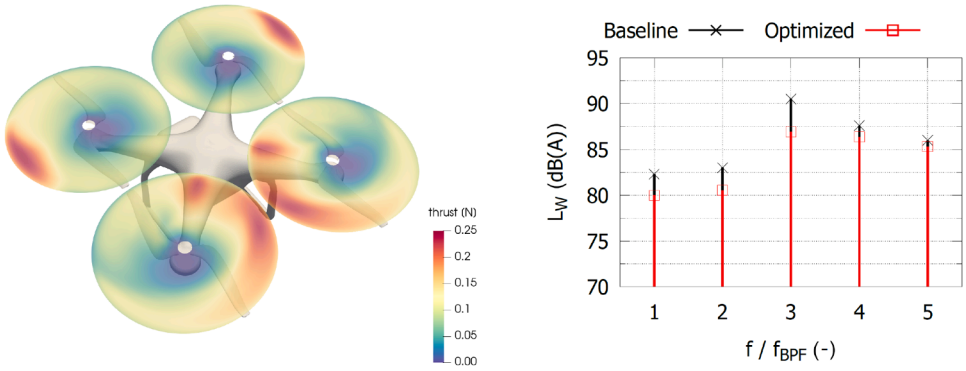

(a) (b)

Fig. 7. (a) Propeller blade loading absolute value for the second optimisation case and (b) A-weighted SWL levels for the second optimisation case.

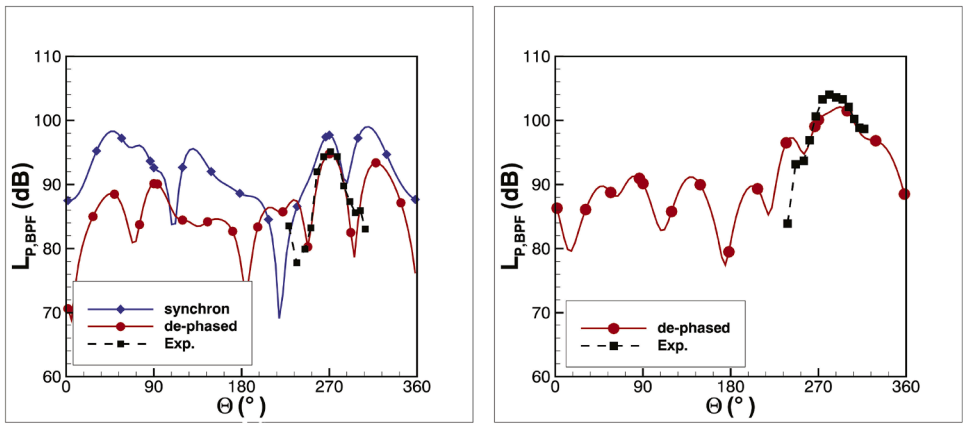

(a) (b)

Fig. 8. Fly-over noise directivity for AoA = 0° (a) and AoA = 10° (b) compared to experimental results.

Written by Berk Sarikaya: berk.sarikaya@iag.uni-stuttgart.de, Institute of Aerodynamics and Gas Dynamics, University of Stuttgart, Germany

3.5. Noise sources of a distributed propulsion system

The study [10] explored the noise sources of a Distributed Electric Propulsion (DEP) system based on a three propeller - wing configuration in a wind tunnel. To identify the dominant tonal noise sources, high-fidelity URANS simulations were conducted with further noise propagation through the FWH analogy. The choice of integration surface made it possible to extract the individual noise sources originating from the propellers or emitted by the wing as a result of interactions. In addition, the numerical results of the presented work were validated with wind tunnel measurements in the aeroacoustic facility of the DNW-NWB.

The work revealed that beside noise generated by the propellers, noise arising from the wing was considerable in several directions, especially for zero Angle of Attack (AoA). Moreover, the influence of the wing's potential field increased significantly the unsteady loading noise of the propellers. In the high-lift case at AoA = 10°, the unsteady loading noise from the propellers predominated, where the upwash of the wing was responsible for this effect.

The validation with experimental data showed good agreement if the relative propeller phases were de-phased, see Fig. 8. Due to interferences, the noise levels of synchronised and de-phased propellers differed significantly. However, the propellers were not synchronised during the tests and the phase angles were not known. Thus, for both angles of attack, good agreement was achieved with the de-phased approach, taking into account all acoustic effects, which include both the active noise sources mentioned and shielding effects by the surrounding structures in the wind tunnel.

Written by Robin Wickersheim: robin.wickersheim@iag.uni-stuttgart.de and Manuel Keßler, Institute of Aerodynamics and Gas Dynamics, University of Stuttgart, Germany

3.6. Overlapping disk effects on tandem propellers noise in hover flight condition

An experimental campaign performed at Politecnico di Milano was aimed to evaluate the aerodynamic interaction effects on noise emission of tandem propellers typical of electric Vertical Take-Off and Landing (eVTOL) aircraft configurations in hover flight [11]. The research activity has been addressed within the framework of the HC/AG-26 "Noise Radiation and Propagation for Multirotor System Configurations", supported by the Group for Aeronautical Research and Technology in Europe (GARTEUR) .[3] The comprehensive test campaign investigated in particular the effects of partial propeller disks overlap on the acoustics signature as well as on the aerodynamic performance of the dual-propeller system. Microphones and aerodynamic loads measurements were performed in an anechoic test chamber, see Fig. 9(a). In addition, Stereo Particle Image Velocimetry (SPIV) surveys combined with mid-fidelity simulations performed using DUST enabled to enhance the comprehension of the interactional flow physics involved in the phenomenon.

The test activity revealed that a partial overlap between propeller disks was responsible of a consistent increase of acoustic footprint of the dual-propeller system that is almost two times greater than the one observed by changing the lateral distance between the propellers without disk overlap. Moreover, blades sense of rotation effect was also investigated, showing that counter-rotating propellers provide a more intense degree of interaction between propellers wakes, leading to a slight increase of the acoustic footprint of the system, see Fig. 9(c). PIVs measurements and DUST simulations results highlighted the occurrence of several Blade-Vortex-Interaction (BVI) events, see Fig. 9(d), that are shown to be responsible for the more severe periodic oscillations experienced by rear propeller blades due to the interaction with the front propeller wake.

The comprehensive experimental database, collected for a not confidential propeller geometry, was considered as a reference benchmark for the validation of aeroacoustic numerical tools with different level of fidelity developed by the European partners participating to HC/AG-26 GARTEUR Group [12].

Written by Alex Zanotti: alex.zanotti@polimi.it, Politecnico di Milano, Italy

4. Acoustic liners and metamaterials

4.1. Converging rainbow trapping silencers for broadband sound dissipation in a low-speed ducted flow

Widely-opened silencers with graded cavity depths are investigated to achieve broadband low-frequency sound dissipation and low drag when traversed by a low speed flow. To reduce both reflection and transmission, these mufflers exhibit rainbow-like sound trapping mechanism with individual cavity resonances activated at frequency-dependent axial locations and slow sound induced by a gradual decrease of their wall admittance [13]. To improve their low-frequency performance and minimise drag, coiled annular cavities with an inner radius following a flow-compliant converging profile was proposed, as seen in Fig. 10(a,b). The acoustic performance of the Converging Coiled Silencer (CCS) were simulated by an analytical Transfer Matrix Method (TMM) validated against two-port scattering matrix measurements and a Thermoviscous Acoustics Finite Element Model in plane wave regime. A causally-guided parametric study showed that a high density of resonators provides impedance matching and near-unit dissipation while a proper selection of the cavities growth rate and coiling factor downshifts the onset frequency for broadband performance. Particle swarm optimisation of the CCS parameters resulted in near-unit dissipation as well as near-zero transmission and reflection as from $k_0 L = 0.58$, the length-based Helmholtz number [14]. Reynolds Averaged Navier-Stokes simulations performed at inlet Mach number $M_{\text{in}} = 0.04$ led to a 2% excess drag with respect to a smooth convergent. Experiments in a low-speed wind tunnel showed that the CCS sound-trapping effect was resilient under Upstream (UPC) or Downstream (DPC) Propagation Conditions, but was Mach number-dependent, as confirmed by the TMM extended to account for convective and dissipative flow effects, as seen in Fig. 10(c–e). DPC reduce the efficiency range of the CCS by upshifting the onset frequency and decreasing the transmission loss (TL) whereas UPC extend the high dissipation plateau towards the low-frequencies while increasing the TL. This study opens up applications like the design of silent convergent nozzles.

Written by Teresa Bravo: teresa.bravo@csic.es, Consejo Superior de Investigaciones Científicas (CSIC), Spain and Cédric Maury, Aix-Marseille University, CNRS, Ecole Centrale Méditerrannée, Laboratory of Mechanics and Acoustics, France.

4.2. Acoustic metamaterial for low frequency range

Classical sound absorbing devices or materials may be classified into two different fields: acoustic resonators (perforated panels, Helmholtz resonators, quarter-wavelength resonators) and porous media. The first solutions can achieve great performance at low frequencies, but only in narrow frequency bands. Porous media, indeed, reach high performance at medium-high frequencies due to nature of their structure (channels, cracks, or cavities within a rigid skeleton, which concretely let the sound waves enter the media and dissipate their energy by viscous and thermal losses). This limitation can be overcome through the use of acoustic metamaterials, which offer great flexibility for manipulating sound. Solutions based on the inclusion of a periodic pattern within a porous material Fig. 11, with the aim of passively improving its acoustic performance in terms of loss of sound transmissions, have been investigated [15].

[3] https://garteur.org/

(a)

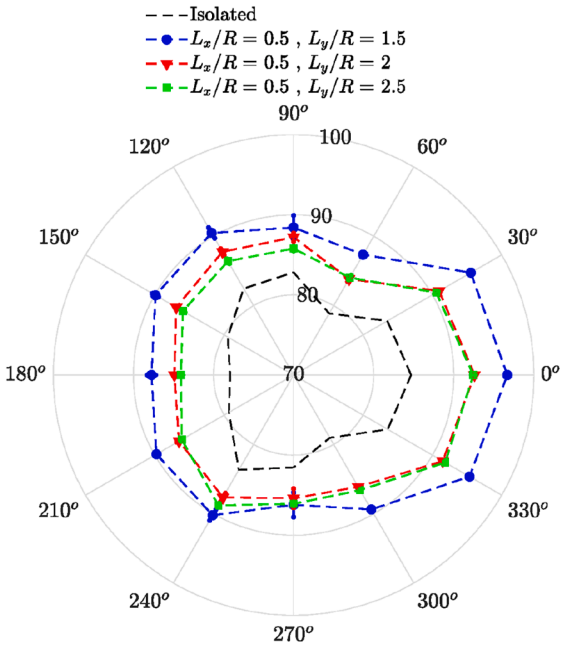

(b)

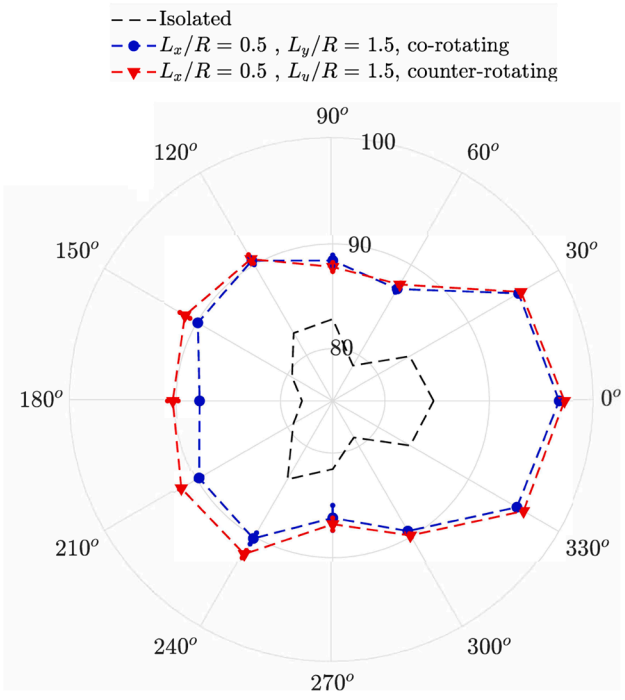

(c)

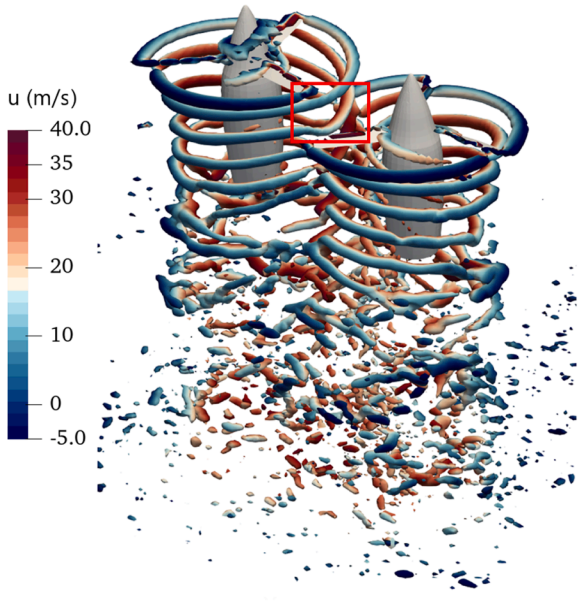

(d)

Fig. 9. (a) Experimental setup; (b-c) comparison of overall averaged SPL at different separation distances and blade sense of rotation; (d) BVI events occurring for overlapped propeller disks configuration with counter-rotating blades highlighted by DUST simulations.

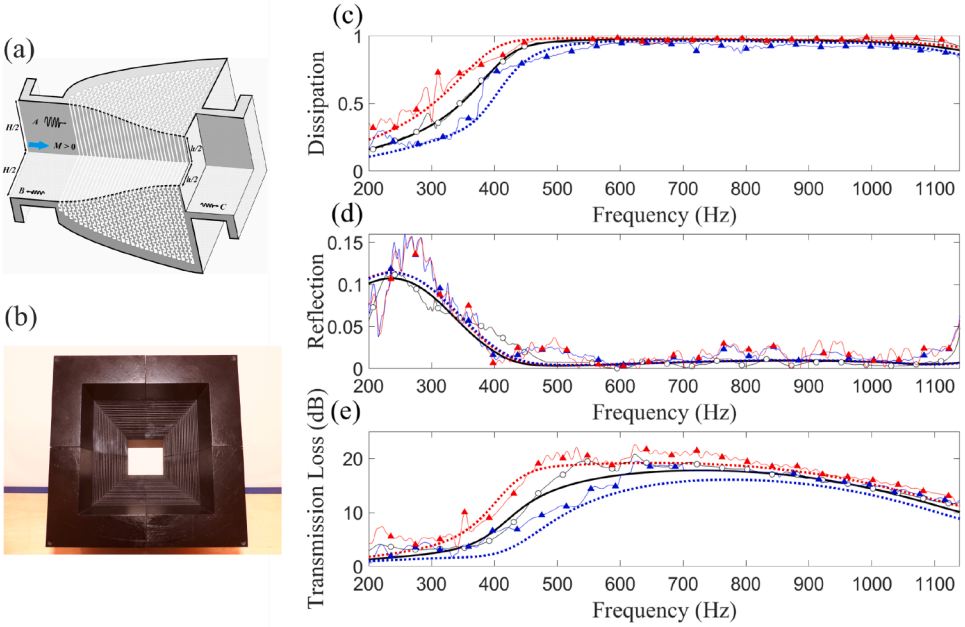

Fig. 10. (a) Sketch of the converging coiled silencer under a left excitation along the flow direction (DPC); (b) Picture of the silencer cavity mouths viewed from the inlet section; (c) Dissipation, (d) reflection and (e) TL spectra of the optimised rainbow-trapping silencer simulated by the TMM (black solid, no-flow; blue dots, DPC: $M_{in} = 0.04$; red dots, UPC: $M_{in} = -0.04$) and measured in the aeroacoustic test bench (white circles, no-flow; blue triangles, DPC: $M_{in} = 0.04$; red triangles, UPC: $M_{in} = -0.04$). (For interpretation of the references to colour in this figure legend, the reader is referred to the web version of this article.)

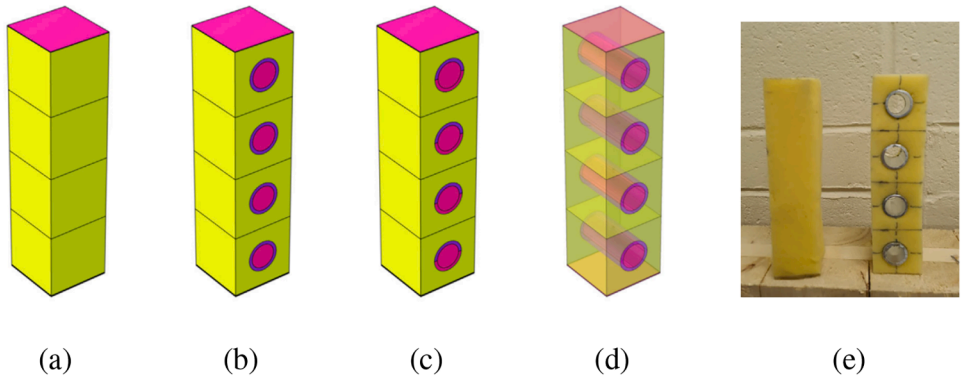

Fig. 11. (a) Homogeneous acoustic package; (b) Hollow inclusions; (c) Half-cut hollow inclusions; (d) Helmholtz resonators; (e) tested sample.

In Fig. 12, it can be appreciated that analytical (TMM), numerical (FEM), and experimental results carried out on configuration 1 are in good agreement, with only some small oscillations in the experimental data at mid-low frequencies. Concerning Configuration 2, the experimental tests show a broad peak brought about by periodicity peak. This is attributed to the fact that the actual damping of the sample is smaller than that estimated by COMSOL MultiPhysics.

The results obtained in terms of Transmission Loss (TL) and Insertion Loss (IL) are presented in Fig. 13. As expected, Configurations 2–4 show periodicity effects that result in increased TL values in a specific frequency range of frequencies, when half of the acoustic wavelength k is equal to periodicity dimension d. Since this kind of acoustic resonance still relates on the thickness of the unit cell, it may be challenging to obtain performance peaks at low frequencies, when only a limited thickness is available. The proposed approach may conceptually be scaled also for low-frequency applications, but only when the total available thickness is sufficiently high, or if it is not considered as a model constraint (generally, both conditions are not applicable to solutions in the field of transport engineering). To improve TL at low frequency, a possible solution is to turn hollow inclusions into Helmholtz resonators (configuration 4).

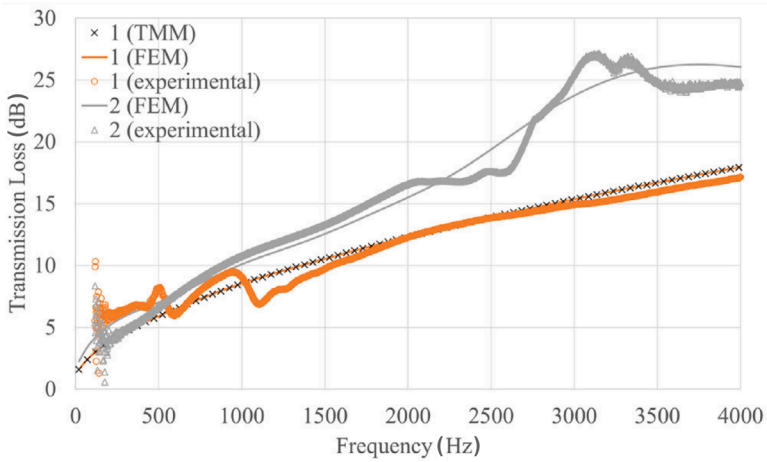

Fig. 12. Numerical and experimental comparison of transmission loss of configurations 1 and 2.

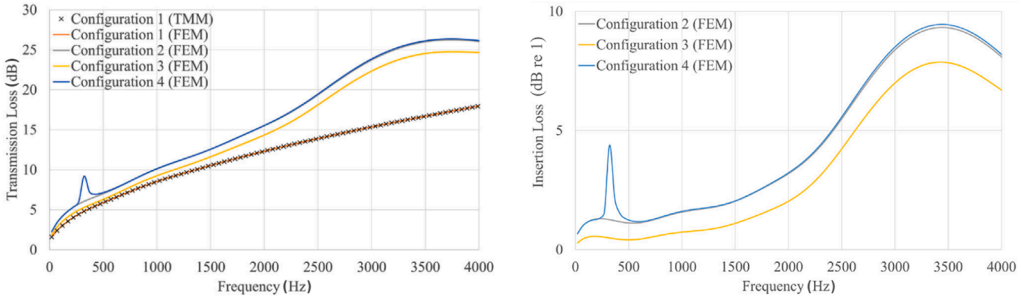

Fig. 13. Numerical transmission loss (a) and Insertion Loss (b) of Configurations from 1 to 4 (TMM and FEM results.).

Written by Giuseppe Petrone: giuseppe.petrone@unina.it, Laboratory For Promoting Experiences In Aeronautical Structures And Acoustics, Università degli Studi di Napoli "Federico II", IT

4.3. MDOF acoustic liner concept with flexible inner wall segment

In recent years, a unique Multi-Degrees-of-Freedom (MDOF) acoustic liner concept has been explored at DLR department of Engine Acoustics and the associated TU Berlin chair of "Turbomachinery- and Thermoacoustics". The proposed liner combines a conventional Helmholtz resonator with flexible cavity walls to obtain more broadband and low-frequency damping (see Fig. 14).

Recently, this concept was experimentally and numerically investigated to separate the effects [16]. Additional microphones implemented inside the resonator allowed us to successfully separate Helmholtz and plate resonances. The numerical study enabled a comprehensive investigation of the impact of the key parameters. These results provide valuable insights into the working principles and highlight the great flexibility of this concept for future optimization and application.

Written by Karsten Knobloch (karsten.knobloch@dlr.de) and Fleming Kohlenberg, DLR Dept. of Engine Acoustics, Berlin

4.4. Optimal design of the edges of perforations to maximise acoustic damping

The acoustic response of circular perforations, such as those found in the acoustic liners of the combustors of gas turbines and rockets and in burners for hydrogen flames, is highly sensitive to modifications of their edges. Straight "short" holes, for which the bias flow within the perforation separates at the inlet and does not have time to reattach prior to the perforation exit, often exhibit acoustic energy amplification - whistling - without any edge modifications. The strong sensitivity to edge modifications was first utilised in [17,18] to design 45° edge chamfers, whose extent was optimised to maximise the acoustic absorption of the perforations. Fig. 15 demonstrates that careful design of these edges can dramatically increase the damping of acoustic energy: the absorption coefficient of two perforations at given frequencies was altered to go from exhibiting strong whistling to strongly damp acoustic energy.

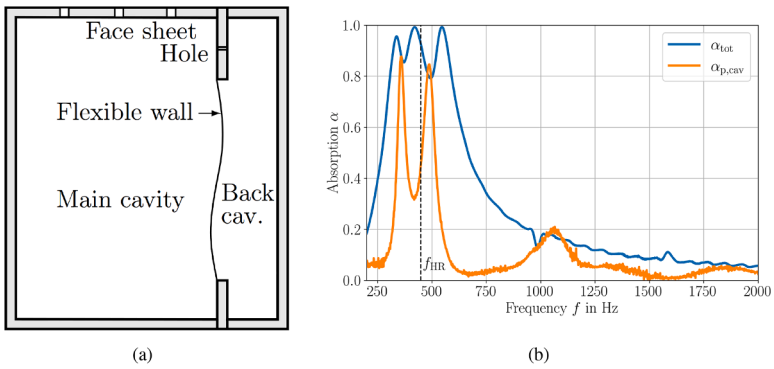

Fig. 14. (a) Schematic cell. (b) Normal incidence absorption of the whole resonator (blue), only the plate with back cavity (orange) determined using cavity microphones and theoretical Helmholtz resonance frequency (black). (For interpretation of the references to colour in this figure legend, the reader is referred to the web version of this article.)

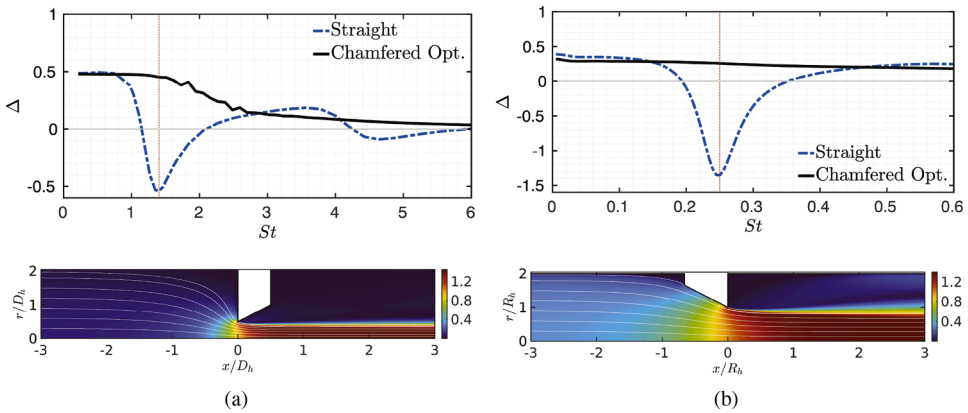

Fig. 15. Acoustic absorption coefficient (top) for straight (blue dash-dotted line) and optimally-chamfered perforation (black solid line). Mean flow velocity magnitude for optimal configurations (bottom). Laminar (a) and turbulent (b) bias flow. (For interpretation of the references to colour in this figure legend, the reader is referred to the web version of this article.)

The design methodology was based on a Bayesian optimisation framework, which can be easily combined with any computational or experimental methodology to characterise the acoustic response of the perforations. In Guzmán-Iñigo and Morgans [17], this was done numerically using an efficient two-step approach: a steady mean flow was first computed using a Newton method, and then the acoustic response was obtained as the solution of the compressible Navier-Stokes equations, linearised about this mean flow. This methodology is suitable for laminar [17] and turbulent flows [18].

The findings obtained through the support of the ERC Consolidator Grant AFIRMATIVE open the door to the bespoke design of the perforations edges in the acoustic liners of gas turbines and rocket combustors and hydrogen burners, reducing their propensity to pernicious thermoacoustic instability and paving the way for the development of safer and greener combustors.

Written by Juan Guzmán-Iñigo: juan.guzman@city.ac.uk, City, University of London, UK, and Aimee S. Morgans, Imperial College London, UK.

4.5. Time-domain simulation of the acoustic nonlinear response of acoustic liners at high sound pressure level

Aircraft engine noise mitigation relies heavily on acoustic liners – typically consisting of perforated plates backed by cavities and functioning as acoustic resonators – which are installed on nacelle walls to absorb and attenuate propagating sound waves. At high SPL, nonlinear effects within these liners significantly influence their acoustic impedance, and thus their performance, while the propagation of sound in the surrounding air can often still be treated linearly. This study addressed the challenge of accurately modeling this nonlinear acoustic response, which becomes important above approximately 130 dB SPL and is strongly influenced by the complex visco-thermal and flow interactions within perforated plate liners.

Building on the Equivalent Fluid Model (EFM) framework, which is widely used to describe wave propagation in porous media, this work – the result of a long-standing collaborative effort between ONERA and ISAE-SUPAERO – extends the EFM to perforated plate liners operating in the nonlinear regime [19]. By incorporating a porous-based description and introducing a nonlinear Forchheimer correction to account for the velocity-dependent resistivity directly in the time domain, the developed model goes beyond classical

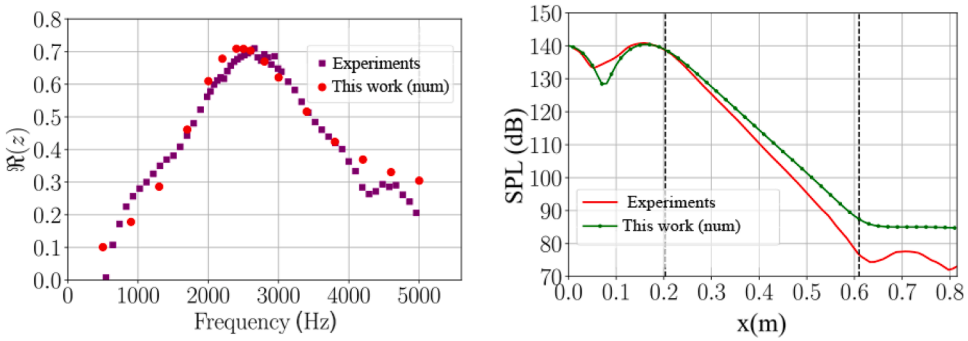

(a) (b)

Fig. 16. (a) Real part of the liner impedance obtained from normal incidence experiments performed at the LAUM laboratory, and (b) numerical results at SPL 150 dB and SPL along the opposite wall to the liner at 1000 Hz in grazing wave conditions, tested by the NASA Langley Liner Physics team, with vertical black dashed lines delimiting the liner position.

frequency-domain impedance boundary condition approaches. The stability of the model was rigorously demonstrated and a practical multipole approximation was constructed to make nonlinear EFM computationally efficient.

Numerical simulations using a discontinuous Galerkin solver showed excellent agreement with experimental results in both normal and grazing incidence configurations, validating the capability of the model to capture nonlinear effects accurately at high SPL, as seen in Fig. 16.

This contribution provides a robust, physics-based tool for designing and optimising advanced aeroacoustic liners, offering the potential to enhance noise reduction strategies in aircraft engines and other demanding applications where high-intensity sound interactions with porous structures play a critical role.

Written by Rémi Roncen: remi.roncen@onera.fr, DMPE, ONERA, Université de Toulouse, 31,000 Toulouse, France

4.6. On the modification of tip leakage noise sources by over-tip liners

Over-Tip-Rotor (OTR) liners have been proposed to further reduce fan broadband noise in turbofan engines. The mechanisms behind OTR noise reduction have been studied in recent years and are summarised in Fig. 17(a). These include: (1) conventional acoustic attenuation, with noise dissipation enhanced by source proximity; (2) acoustic back-reaction effects on the source; and (3) modifications to the unsteady tip flow and related noise. Palleja-Cabre et al. [20] experimentally investigated tip-leakage noise reduction using OTR liners. The setup involved a static aerofoil with its tip positioned over a flat plate containing a liner insert, separated by a small gap. OTR liners primarily reduced high-frequency tip-leakage noise through *acoustic* back-reaction effects, which can be tuned via liner design and qualitatively predicted with simple analytical models, Fig. 17(b). For the first time in the literature, experimental results confirmed that OTR liners alter the unsteady wall pressure at aerofoil tip locations critical to tip-leakage noise generation. These reductions in tip wall pressure were found to correspond to peak far-field noise reductions, Fig. 17(c), with the coherence between wall pressures and far-field noise dropping significantly when an OTR liner was installed. It was also demonstrated that OTR liners can modify the tip-leakage flow, weakening coherent flow structures responsible for low-to-mid-frequency tip-leakage noise, thereby causing a hydrodynamic source modification.

Written by Sergi Palleja Cabre: s.palleja-cabre@soton.ac.uk, Institute of Sound and Vibration Research, University of Southampton, UK

5. Experimental techniques in aeroacoustics

5.1. Deformable-boundary integral formulation for the solution of arbitrarily-forced acoustic wave equation

The propagation of perturbations in fluids is governed by an acoustic wave equation. An arbitrarily-forced wave equation is introduced in [21] which, properly adapted, gives rise to equations describing specific phenomena of signal perturbation propagation in fluids (like, for instance, the Lighthill and Ffowcs-Williams and Hawkings equations for radiation and scattering). Then, its solution is determined through a novel boundary integral formulation based on the free-space Green function, which is applicable to fluid domains bounded by solid or porous deformable surfaces. Different versions of the proposed boundary integral formulation are derived, depending on the frame of reference in which they are expressed [21]. The numerical investigation begins with the comparison of the results obtained by the presented formulation against analytical solutions concerning both a pulsating solid sphere and a deformable porous surface that encloses pulsating sources. Then, the equivalence of the formulations expressed in different frames is examined for a bending and twisting non-lifting wing translating at different Mach numbers. Finally, the aeroacoustic field generated by a helicopter rotor model in forward flight is examined to assess the effect of the body deformation on the radiated noise and the accuracy of the numerical simulations by comparison with experimental data. The results of the numerical investigation have provided a

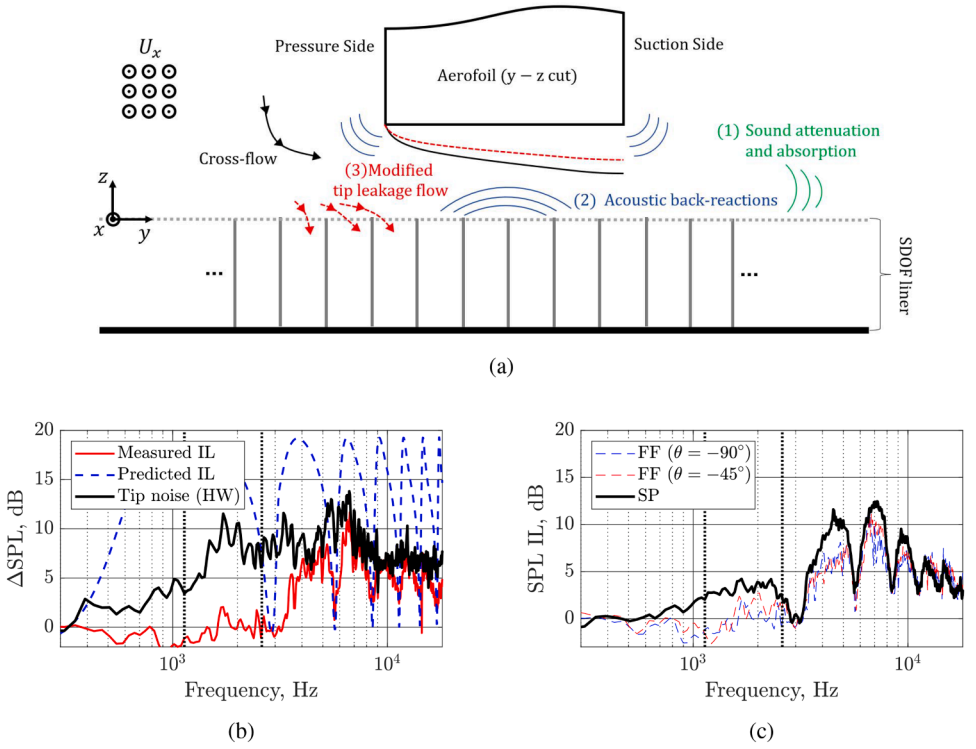

Fig. 17. Noise reduction with over-tip liners; (a) schematic of the proposed noise reduction mechanisms, (b) measured and predicted far-field SPL Insertion Loss (IL) and comparison to tip leakage excess noise of the hard wall (HW) configuration, and (c) comparison of wall pressure (SP) and far-field (FF) SPL insertion loss at two azimuthal θ locations.

comprehensive validation of the deformable-boundary integral formulation presented for the analysis of wave propagation in fluids, and confirmed its capability to study problems of engineering interest [21].

Written by Massimo Gennaretti: massimo.gennaretti@uniroma3.it, Department of Civil, Computer Science and Aeronautical Technologies Engineering, Roma Tre University, Rome, Italy

5.2. Semi-empirical calibration of remote microphone probes using Bayesian inference

Remote Microphone Probes (RMP), such as pinhole-mounted ones, are often calibrated empirically, e.g. with plane-wave tube calibrators. These calibration processes introduce *spurious* resonance, related to the calibrator geometry, in the estimated frequency response of the probe, i.e. its Transfer Function (TF). If not corrected, this spurious resonance propagates to any unsteady pressure measurements to which the TF is applied. Manually post-processing this calibration can itself introduce errors, as its accuracy entirely depends on the expertise of the operator.

The ASSIST (BAyesian proceSsing of SpurIous reSonance in calibraTion data) method was developed to remove this spurious resonance in a less operator-reliant manner [22]. This is achieved by considering not only the measured TF, as is the case with manual post-processing, but also the approximate dimensions of the probe, which informs an expected TF based on an analytical TF model, as illustrated in Fig. 18. The fitting is performed by means of Bayesian inference, i.e. Markov-chain Monte Carlo. The underlying code has been made publicly available through an online repository [23]. This code implementation of the analytical TF model can be additionally used to design and optimise the RMP geometry for a specific experimental campaign.

ASSIST has been used to successfully process different example datasets, generated by pinhole-mounted microphones and a microphone mounted in a semi-infinite waveguide-type RMP. Compared to manual processing techniques, the method reconstructs the frequency bands of the TF affected by spurious resonance with a physically correct alternative. All resonance that is physical to the probe is retained, while strongly reducing the impact of operator expertise on the final processed TF and the resulting calibrated unsteady pressure measurements. Furthermore, the values of the fitting parameters that best reflect the actual probe geometry can be used for corrective models, e.g. to account for the effect of the grazing flow over the microphone probe orifice and flow temperature on its TF.

Written by Olivier Moriaux: o.k.m.moriaux@tudelft.nl, Riccardo Zamponi and Christophe Schram, Von Karman Institute for Fluid Dynamics, Belgium.

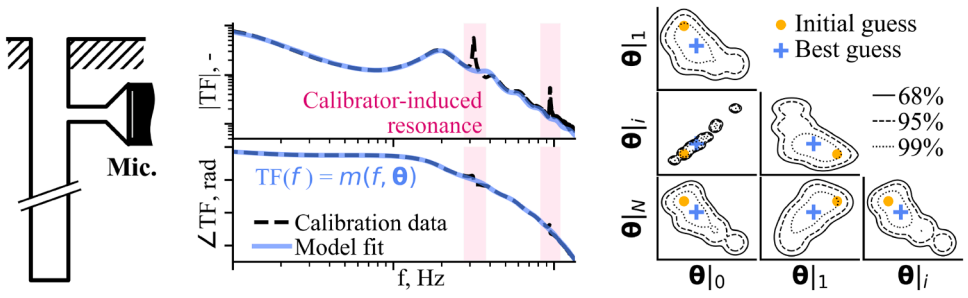

Fig. 18. Illustration of the ASSIST method applied to RMP calibration data. a) Diagram of a semi-infinite waveguide type RMP. b) Empirical TF with spurious resonance and model fit from the ASSIST model. c) Highest density credible intervals of some model parameter combinations with the initial and best guesses for the parameter values.

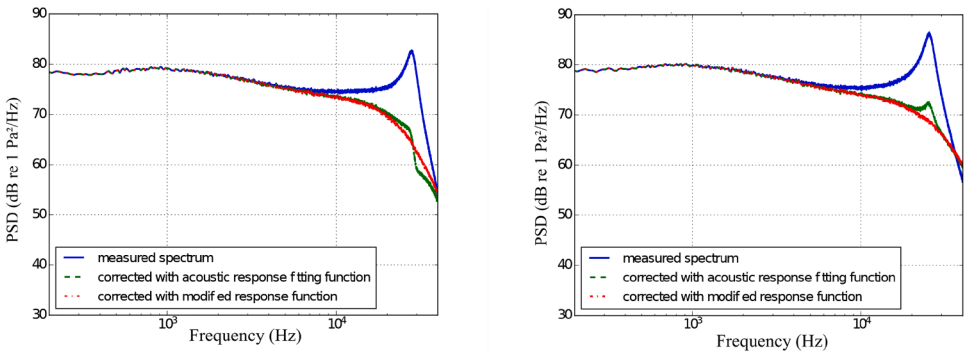

Fig. 19. Measured and corrected wall pressure spectra in zero pressure gradient flows with $U_\infty = 60$ m/s, (a) $d = 0.5$ mm (b) $d = 0.35$ mm.

5.3. Flow effect on measured wall pressure spectra by pinhole-mounted sensors

Wall pressure fluctuations were measured on a flat plate using pinhole-mounted Kulites with different pinhole diameters and cavity volumes [24]. The acoustic response functions of the pinhole-mounted Kulites were determined with a laser plasma generated sound source. Fig. 19 shows the measured and corrected wall pressure spectra using acoustic calibration determined transfer function and modified transfer function where the damping factor and resonance frequency were adjusted. Fig. 20 shows the ratio of the adjusted parameters relating to the acoustic determined parameters, scaled with $\omega_r d/U_c$. The convection velocity U_c represents the velocity of wall pressure fluctuations passing over the pinhole, which is pinhole size and flow condition dependent, i.e. the value changes significantly with flow pressure gradients, which were produced by placing a NACA 0012 airfoil above the plate. The ratio of the damping factor in flow and without flow, D_f/D_a, between each sensor configuration cross at the frequency $\sqrt{2}$ times larger than the frequency at the minimum value of D_f/D_a. This feature may indicate that a flow-induced resonance is superposed to the Helmholtz resonance. It is assumed that the Rossiter mode is induced when the first mode frequency coincides with the Helmholtz resonance frequency. The results showed that the spectra can be well-corrected in practice using the same formula for the Helmholtz resonance excited by acoustic sources with modified damping factor and resonance frequency.

Written by Nan Hu: nan.hu@dlr.de, German Aerospace Center (DLR), Germany

6. Urban air mobility related noise

6.1. A minimum objective function trim procedure for VTOLs noise reduction

A novel approach for multi-rotor acoustic nuisance mitigation based on the identification of optimal control settings is proposed in Poggi et al. [25]. This strategy is possible thanks to the peculiarity of multi-rotor systems (e.g., those involved in urban air mobility applications) to have redundant controls. The idea is to take full advantage of the control redundancy by defining the control settings that guarantee the desired steady-state flight conditions while, at the same time, optimising selected target functions such as performance or noise emissions. To this aim, the trim problem is recast into a constrained cost function minimisation problem. Since the objective is to reduce as much as possible the noise disturbance of trimmed VTOL, an aeroacoustic tool based on the chordwise-

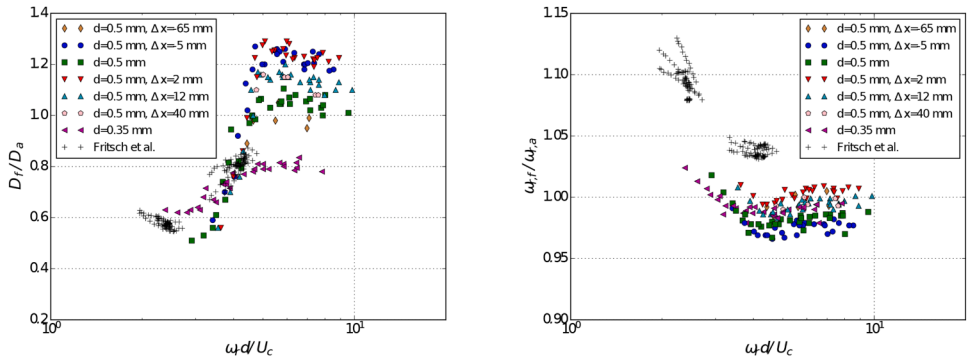

Fig. 20. Ratio of (a) damping factor (b) resonance frequency for excitation by turbulent boundary layer flows and acoustic sources scaled with $\omega_r d/U_c$.

compact form of the Farassat 1A formulation for the evaluation of noise radiation is suitably coupled with a trim solver [25]. The numerical investigations consider quadcopter and hexacopter configurations in level flight at several advancing speeds. Comparisons of the proposed minimum-noise trim strategy with two other trim strategies based on the minimisation of rotor torque and control effort prove its capability to provide an overall reduction of noise throughout the entire velocity range examined.

Written by Caterina Poggi: caterina.poggi@uniroma3.it, Department of Civil, Computer Science and Aeronautical Technologies Engineering, Roma Tre University, Rome, Italy

6.2. Low-noise fan design and sound quality assessment for distributed propulsion systems

For low-speed fan stages, tonal rotor-stator interaction noise is typically the dominant noise source, especially for fan stages with fewer stator than rotor blades, i.e. low-count OGV (Outer Guide Vane) fans.

Two tonal noise reduction mechanisms for low-count OGV fans were analytically, numerically, and experimentally verified [26]. Firstly, an inverse cut-off of the blade passing frequency tone presents a promising mechanism for tonal noise reduction. This effect is restricted to low-speed, low-count OGV fans, as a cut-off condition can be realised with fewer stator vanes than rotor blades only if the rotor tip Mach number is low enough. A design rule is, therefore, derived to estimate the limiting rotor tip Mach number. Secondly, for low-count OGV fans, which do not achieve the cut-off condition, an additional effect is evaluated that mitigates tonal noise excitation, even if the BPF is cut-on. The physical mechanism is linked to the propagation direction of the excited acoustic waves relative to the dipole radiation axis. When the propagation direction of the dominantly excited acoustic mode is perpendicular to the dipole radiation axis, a minimum of acoustic energy is excited. To ensure the application of this effect, a design rule was derived. The tonal noise reduction potential and sound quality impact of these effects is demonstrated on two low-count OGV fan stages (see "low-tone" and "low-broadband" in Fig. 21). A major characteristic of these fan designs is that the aerodynamic performance and the psychoacoustic loudness values are similar, while showing differences for other sound quality metrics. Thus, these fans are well-suited for psychoacoustic assessments.

In Schade et al. [27], the acoustic interactions due to rotational speed deviations were investigated for a UAM vehicle powered by 26 distributed fans, following the low-broadband design from Fig. 21. Synthesised fly-over sounds were generated for different ranges of rotational speed deviations, and the impact on noise immission and psychoacoustic sound quality metrics were assessed, see Fig. 21. The study indicates that temporal fluctuations decrease in amplitude with increasing rotational speed deviations, resulting in lower values for loudness, tonality, and fluctuation strength.

Written by Stephen Schade: stephen.schade@dlr.de, German Aerospace Center and Roberto Merino-Martinez, Delft University of Technology.

7. Miscellaneous

7.1. Turbulent flow characteristics and noise implications downstream of an automotive radiator

The turbulent flow characteristics downstream of an automotive radiator were investigated through SPIV [28], with a focus on turbulence production, dissipation, non-homogeneity, and anisotropy. The turbulent flow past the radiator plays a key role in turbulence-interaction noise when it encounters the downstream low-speed cooling fan illustrated in Fig. 22(a). The study evaluates the applicability of turbulence models, typically based on assumptions of isotropy and homogeneity, for predicting noise emissions.

To better understand the flow behaviour downstream of the radiator, the research also considers the influence of a circularly-perforated wood panel, designed to simulate the contraction of streamlines caused by the fan casing. Various methods were used to quantify the flow's non-homogeneity and anisotropy. The results show that in the region where the downstream fan would typically

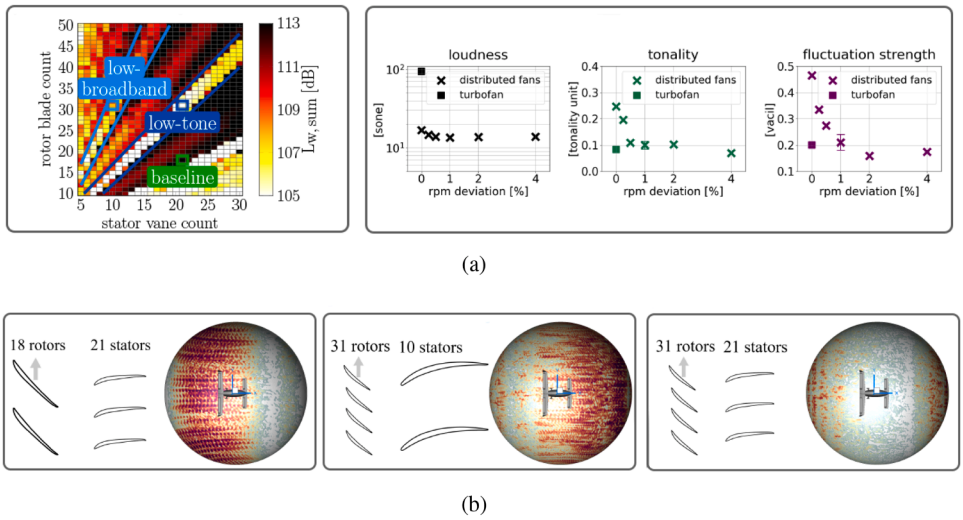

Fig. 21. a) Tonal interaction noise levels for different rotor / stator blade counts and impact of rotational speed (rpm) deviations on Sound Quality Metrics for the low-broadband fan. b) 2D cross-sections of three selected fan designs (left: baseline, center: low-broadband, right: low-tone) and tonal noise directivities obtained from a distributed propulsion system plotted as hemispheres.

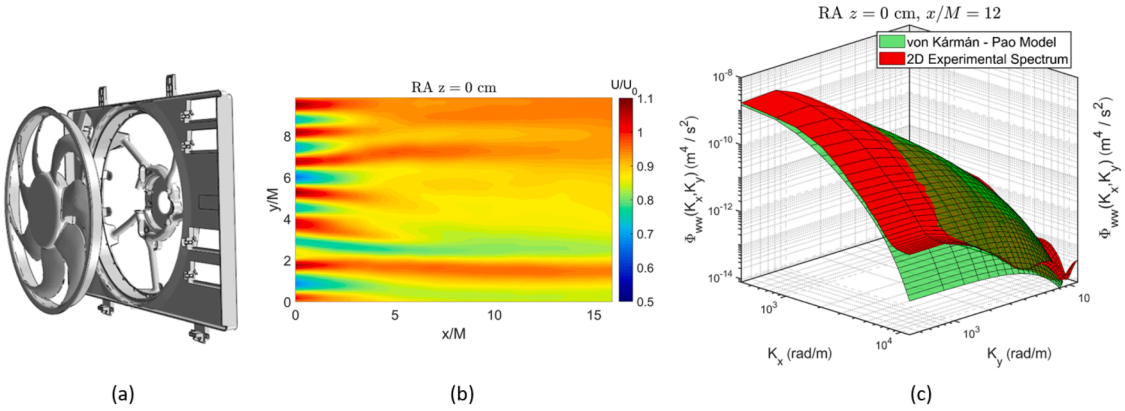

Fig. 22. Automotive low-speed cooling fan (a); SPIV streamwise velocity component highlighting the radiator fins' wakes (b); von-Kármán-Pao-corrected turbulence spectrum compared to the experimentally measured one (c).

be located ($x/M = 12$ in Fig. 22(b)), the flow exhibits significant transverse non-homogeneity, primarily due to wakes generated by the radiator fins. While the flow in this region is not isotropic, a gradual trend toward isotropy emerges, particularly in the presence of the wood panel contraction, which accelerates the flow.

Compared to studies on heat exchangers with wider gaps between cooling pipes, the fins and louvers of the radiator core primarily disrupt vortical structures rather than generating large eddies. This explains the relatively low turbulence intensity levels measured in these flow conditions. The von Kármán turbulence model, which is typically used as input to broadband fan noise modeling, provides a reasonable approximation of the two-dimensional experimental turbulence spectrum. This is obtained when exponentially correcting the spectrum (Pao's correction) at high wavenumbers, as shown in Fig. 22(c). Nevertheless, caution is advised when employing it in noise prediction cases involving rapid flow acceleration, such as that induced by the wood panel contraction.

Written by Alessandro Zarri: alessandro.zarri@vki.ac.be, von Karman Institute for Fluid Dynamics, Belgium

7.2. Experimental application of pseudo-equivalent deterministic excitation method through an impact test

The prediction of the vibrational response of a structure subjected to an aerodynamic load is fundamental for assessing preliminary structural design and addressing typical structural problems such as fatigue and structure-borne sound. Wind tunnel facilities are mandatory to test the structure design efficiency or to analyse new material performances under aerodynamic load, but these tests can be expensive and take a long time to set up and operate. In the paper [29], an alternative approach the eXperimental Pseudo-Equivalent Deterministic Excitation Method (X-PEDEM) is presented. PEDEM takes the main concept of modal decomposition applied

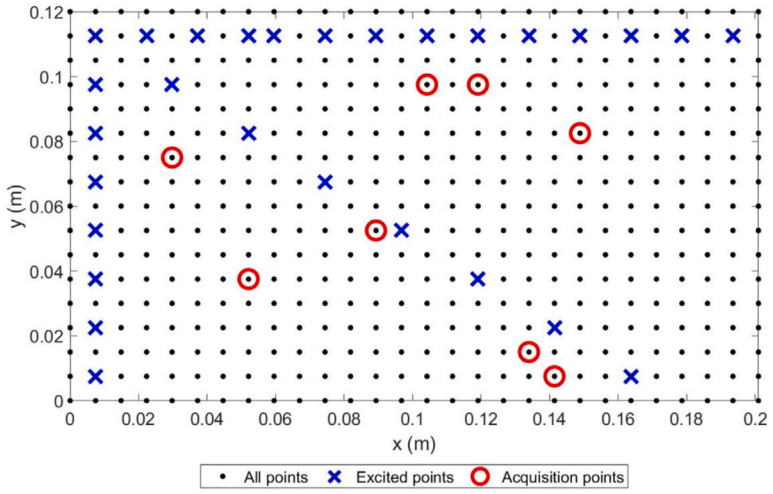

Fig. 23. Configuration for the position of excitation points (blue crosses) and for acquisition points (red circles) over a generic mesh grid of a panel. (For interpretation of the references to colour in this figure legend, the reader is referred to the web version of this article.)

from the Pseudo Excitation Method (PEM), individuating eigenvectors and eigenvalues of the load Cross-Spectral Density(CSD) matrix, and bypassing the actual modal computation by considering two asymptotic representations of the Turbulent Boundary Layer (TBL) CSD matrix eigensolutions–in Low-Frequency (LF) and High-Frequency (HF) domains. In view to demonstrate the capabilities of the method, an experimental hammer test campaign was conducted on three aluminum panels with varying boundary conditions and asymptotic flow velocities. For X-PEDEM applications in the HF domain, both acquisition and excitation points can be chosen randomly, while to cover the LF domain, it is important to ensure the spatial correlation of the excitation over the surface of interest. After a trial and error process, it was found out that the best configuration for the position of the excitation points is the one shown in Fig. 23.

As first experimental validation of X-PEDEM, the numerical FSR (Frequency Spectral Response) obtained with the Corcos model is considered here as reference solution. The structural response of the tested panel PAN A has been evaluated for three different asymptotic flow velocities, for which three different coincidence convective frequencies are identified. The coincidence convective frequency is reported here since it is considered an approximated indicator of the frequency region limit for X-PEDEM; in particular, the X-PEDEM post-processing in LF domain is valid below f_c, while the X-PEDEM post-processing in HF domain is valid above f_c. X-PEDEM solutions have been first calculated numerically and they are shown together with the experimental application of X-PEDEM to the hammer test measurements. In Fig. 24, it is possible to appreciate that both numerical and experimental X-PEDEM results can represent, in an optimal way, the reference solution for all three asymptotic flow velocities. More precisely, it can be seen that numerical X-PEDEM solutions can match the reference one for those frequencies that are far from the convective coincidence frequency f_c. Indeed, both methodologies loose accuracy around this frequency, resulting in an underestimation of the solution. The experimental X-PEDEM presents this underestimation too; it can be argued that a difference between an experimental result and its numerical calculation is always expected, since several factors can influence the experiment performance, such as the sensibility of the sensors, the replication of the boundary conditions, and even the human performance of an impact test.

Written by Giuseppe Petrone: giuseppe.petrone@unina.it, Laboratory For Promoting Experiences In Aeronautical Structures And Acoustics, Università degli Studi di Napoli "Federico II", IT

Written by Jan Delfs: Jan.Delfs@dlr.de, German Aerospace Center, Institute of Aerodynamics and Flow Technology, Germany

Written by Denis Gély: denis.gely@onera.fr, ONERA, France and Jan Delfs, German Aerospace Center, Institute of Aerodynamics and Flow Technology, Germany

Written by Luminița Drăgăşanu: luminita.dragasanu@comoti.ro, COMOTI - Romanian Research and Development Institute for Gas Turbines, Bucharest, Romania.

7.3. Turbulence distortion and leading edge noise

The distortion of turbulence interacting with thick airfoils has been analysed by Piccolo et al. [30] to investigate its impact on leading edge noise generation and prediction. The Lattice-Boltzmann method-based software PowerFLOW has been used to investigate the interaction of grid-generated turbulence with a NACA 0012 and a NACA 0012–103, featuring the same thickness distributions but different leading edge radii.

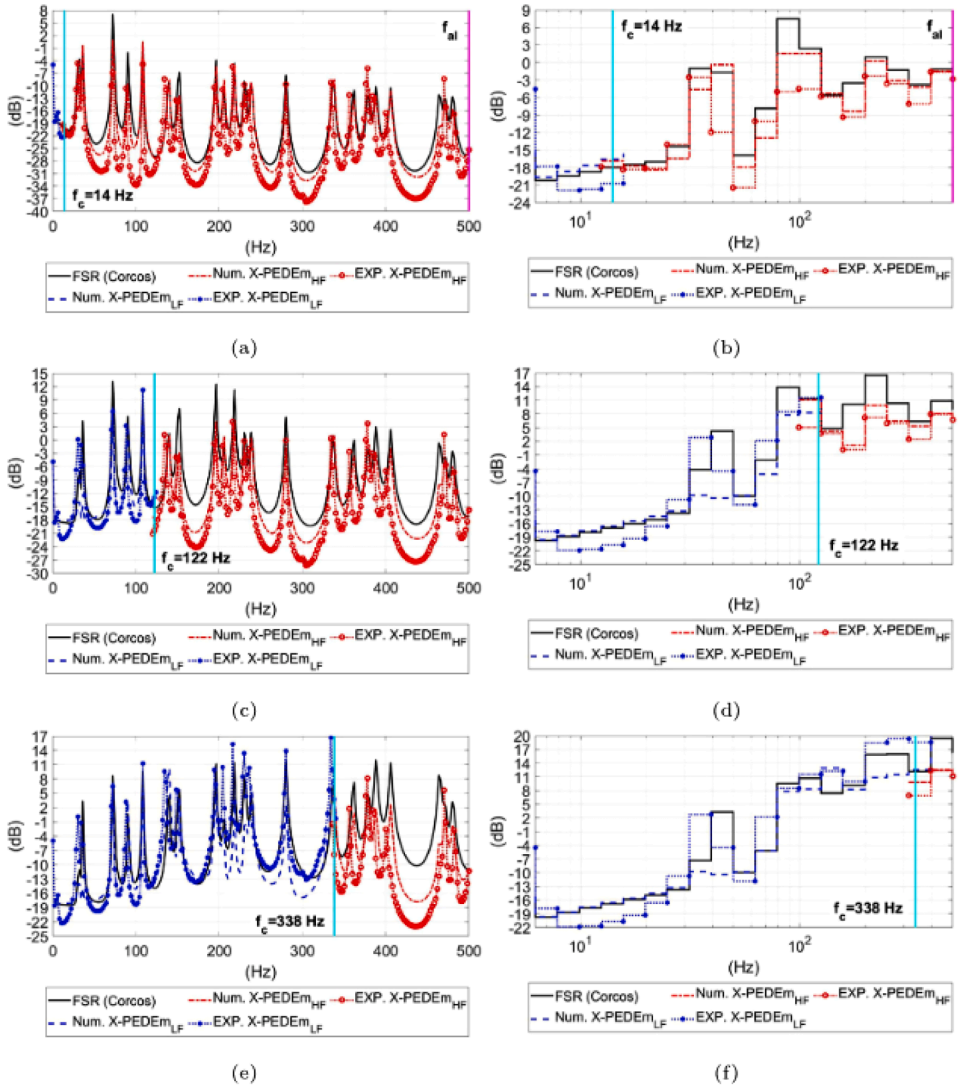

Fig. 24. Panel PAN A (all edges free): structural response (PSD acceleration) to a TBL excitation (Corcos model) at different flow velocities U_0. Comparison between the numerical FSR (solid line), numerical X-PEDEM applied in the LF (dashed line) and HF domain (dotted-dashed line), experimental X-PEDEM for the LF (dotted line with full circle) and HF domain (dotted line with empty circle) evaluated for $N_{acq} = 8$ and $N_{ex} = 16$. (a) narrow bands for $U_0 = 25\ m/s$ (fc = 14 Hz); (b) 1/3 octave bands for $U_0 = 25\ m/s$ (fc = 14 Hz); (c) narrow bands for $U_0 = 75\ m/s$ (fc = 122 Hz); (d) 1/3 octave bands for $U_0 = 75\ m/s$ (fc = 122 Hz); (e) narrow bands for $U_0 = 125\ m/s$ (fc = 338 Hz); (f) 1/3 octave bands for $U_0 = 125\ m/s$ (fc = 338 Hz).

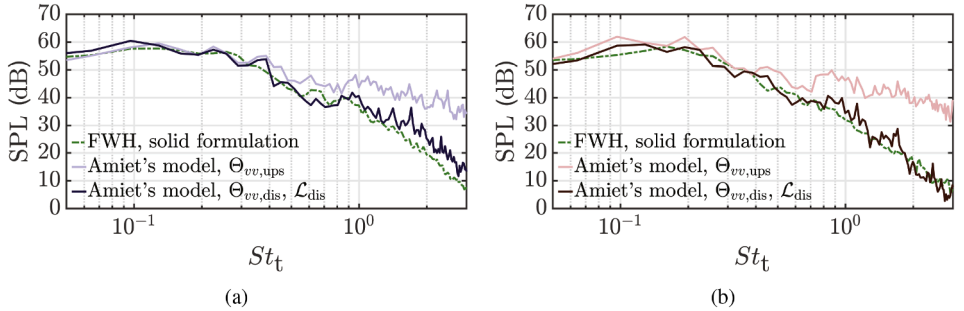

Fig. 25. SPL for an observer placed above the leading edge (R = 1.2 m, $\theta = \pi/2$), for the (a) NACA 0012 and the (b) NACA 0012-103 airfoils. Amiet's model implementations using the upstream spectrum $\Theta_{vv,\mathrm{ups}}$ and the distorted spectrum $\Theta_{vv,\mathrm{dis}}$ along with the corrected aeroacoustic transfer function $\mathcal{L}_{\mathrm{dis}}$ are compared to the results of the FW-H analogy. The reference pressure used to calculate the SPL is 2×10^{-5}Pa.

Fig. 26. The main hall of the University Roma Tre.

The velocity field alteration in the stagnation region has been found to be consistent with the analytical results of Rapid Distortion Theory (RDT). The deformation of large-scale turbulence induced by the surface blockage causes the amplitude of the upwash velocity fluctuations to increase in the low-frequency range of the spectrum. In contrast, the distortion of small-scale structures leads to an exponential decay of the spectrum at high-frequencies as a result of vorticity deformation. The prevalence of one distortion mechanism over the other depends on the size of the turbulent structures with respect to the distance between the stagnation point and the curvilinear abscissa where surface-pressure fluctuations, pressure gradient, and the curvature derivative peak. The identification of this characteristic dimension, which corresponds to the cylinder radius in the original formulation of the theory, allows the extension of the RDT results to airfoil geometries. Surface-pressure spectra in the leading edge region feature the same high-frequency exponential-decay slope, suggesting that the distorted velocity field induces the airfoil unsteady response. In view of the above, the effects of realistic geometry can be fully encompassed in Amiet's model by using a distorted turbulence spectrum $\Theta_{vv,\mathrm{dis}}$ obtained at the stagnation point. This adjustment necessitates modifying the acoustic response to reflect the altered energetic content of the distorted turbulence term, which can be achieved by scaling the aeroacoustic transfer function. The proposed approach results in an accurate noise prediction for both airfoils, capturing both the high-frequency decay slope and the overall noise levels, as shown in Fig. 25.

Turbulence-distortion effects should thus be estimated in the immediate vicinity of the stagnation point to be incorporated into Amiet's model. This identifies a more robust approach than that currently proposed in the literature, which relies on the identification of a representative sampling location where to extract turbulence statistics. At the stagnation point, distorted-flow conditions can be predicted with the RDT, only requiring knowledge of the upstream undistorted turbulence intensity and integral length scale and the body characteristic dimension.

Written by Andrea Piccolo: a.piccolo@tudelft.nl, Technische Universiteit Delft, The Netherlands

8. Conferences and events

8.1. 30th AIAA/CEAS aeroacoustics conference 2024 in Rome

From June 4, to 7, 2024, Rome hosted the 30^{th} edition of the AIAA/CEAS Aeroacoustics Conference, Aeroacoustics 2024.[4] The University of Roma Tre and the Italian Association for Aeronautics and Astronautics (AIDAA) managed the organisation of the event. The technical sessions were held in the classrooms of the Department of Humanities at Roma Tre, while the plenary lectures took place in the Aula Magna, capable of accommodating over 500 people.

The conference set records: an exceptional number of more than 520 abstracts were submitted, of which around 500 were accepted. More than 90 filed for the "Best Student Paper" award. The number of participants was 574. Four plenary lectures took place: two keynotes were given by high-ranked representatives of the aerospace industry, the other two were dedicated to the winners of the highly prestigious "CEAS-Aeroacoustics Award" (Pieter Sijtsma) and "AIAA-Aeroacoustics Award" (Krishnamurthy K. Viswanathan). In addition to the technical sessions, the conference included two workshops on Fan Broadband Noise and Hybrid Wind Tunnels. Social events took place at the prestigious venues in the heart of Trastevere, and at Palazzo Brancaccio. The organisation of the conference was managed by Professor Roberto Camussi of the University of Roma Tre, then chair of the ASC (Aeroacoustic Specialists' Committee) of CEAS, in collaboration with Professor Francesco Marulo of the University of Federico II in Naples, representing AIDAA, and with support from Kent Gee, professor at Brigham Young University and delegate of the AIAA Technical Committee (Fig. 26).

[4] https://www.aidaa.it/aeroacoustics/

Fig. 27. Jan Delfs, Denis Gély, Phil Morris AIAA-CEAS Aeroacoutics Conference, Roma, 2024.

8.2. Ceremony of the 30th anniversary AIAA-CEAS aeroacoustics conference

The thirtieth anniversary of the joint AIAA/CEAS Aeroacoustics Conference was celebrated in Rome, June 2024. Phil Morris (AIAA), Jan Delfs and Denis Gély (CEAS) recalled briefly the history of the joint AIAA/CEAS Aeroacoustics Conference. In the eighties, several European aeroacousticians used to attend the AIAA Aeroacoustics Conferences which gathered 100–150 people. At that time in Europe, there were various national institutes or societies for aerospace sciences but no unified European structure. Then, CEAS was created in the beginning of the nineties. In 1993, the Aeroacoustics Specialists' Committee of CEAS was initiated by Hanno Heller representing the German Aerospace Society DGLR. Gérard Fournier and Luigi Morino, as representatives of the French and Italian societies, AAAF and AIDAA respectively, contributed to realise this cooperation dedicated to serve the aeroacoustics community in Europe, under the roof of CEAS. One main task for the new ASC was to contact the AIAA Aeroacoustics Technical Committee AATC for future cooperation, in particular to organise the aeroacoustics conferences jointly, to be held in the USA and in Europe alternately. The negotiations were successful and two years later Hanno Heller from CEAS organised the first joint AIAA/CEAS-Aeroacoustics Conference in Munich, in 1995, in co-chairmanship with Donald Hanson on the AIAA side. Since 1995, the joint conference has been held annually, alternating between the USA and Europe, which now attracts 400–500 participants. It has become the leading international conference in the field of aeroacoustics, focusing mainly on the aerospace domain (Fig. 27).

8.3. 25th Workshop of CEAS-ASC Airframe noise reduction - needs, challenges & opportunities

The 25^{th} CEAS-ASC Workshop was organised by COMOTI - Romanian Research and Development Institute for Gas Turbines and took place in Bucharest, Romania, on the 22^{nd}-23^{rd} of October, 2024.[5] After engine noise, airframe noise is regarded as being the next important noise source that influences overall aircraft-generated noise. While take-off noise is mainly dominated by engine noise, landing noise is characterised by both engine and airframe noise sources, the latter being especially dominant for the largest aircraft. This workshop addressed some main topics, while also being open to discussing others: understanding the physics of airframe noise generation; noise reduction of high-lift devices and landing gears; low noise by design approach; add-on passive and active noise reduction technologies; experimental and numerical approaches.

A total of 42 participants attended the event, representing 23 institutions from 10 countries (France, United Kingdom, Hungary, Romania, Netherlands, Ireland, Germany, Belgium, Italy, and Japan). Four Keynote presentations were included in the program, given by prominent field experts: Eric Manoha (ONERA), Coordinator of the EU Project INVENTOR (INnoVative dEsign of iNstalled airframe componenTs for aircraft nOise Reduction), with the presentation "INVENTOR Overview"; Leonidas Siozos-Rouzoulis (EC/CINEA), Project Officer of the INVENTOR EU Project, with the presentation "The contributions of INVENTOR to H2020"; Mitsuhiro Murayama (Leader, Working Group for the 5th Medium-to-Long-Term Plan, Aviation Technology Directorate, JAXA), with the presentation "JAXA's Research Activities Toward Airframe Noise Reduction". Furthermore, the industry perspective was jointly laid-out by representatives of three renowned aerospace entities: Aline Scotto (Airbus), Vincent Fleury (Dassault-Aviation), and Amine Ghouali (Safran Landing Systems), with the fourth Keynote presentation "Needs, challenges and opportunities in the field of airframe noise". Overall, the workshop provided an opportunity to share research findings, discuss challenges, and foster collaborations within the Aeroacoustics community in Europe, while exploring the potential for international co-operation (Fig. 28).

[5] https://comoti.ro/airframe-noise-reduction/

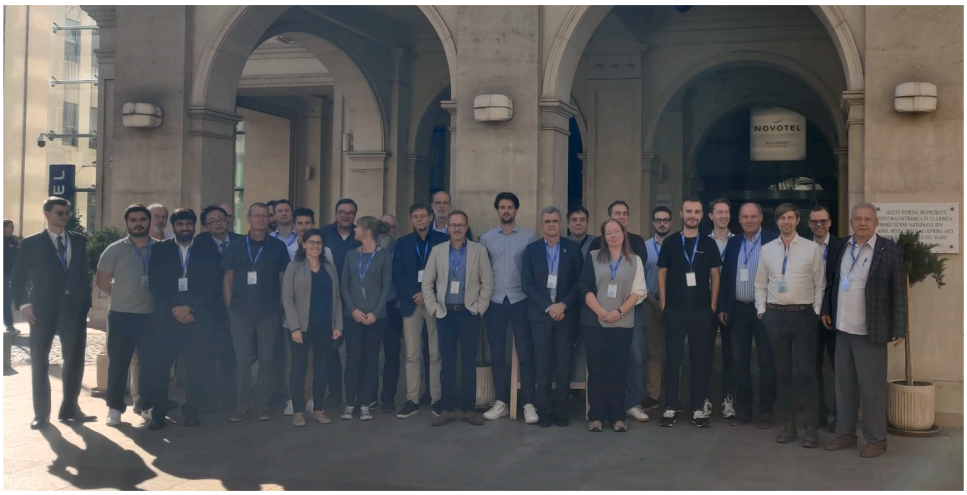

Fig. 28. Group picture of the 25th CEAS-ASC Workshop, 22ndnd-23rd October, 2024, Bucharest, Romania.

CRediT authorship contribution statement

Luminiţa Drăgăşanu: Writing – review & editing, Writing – original draft, Conceptualization; **Damiano Casalino:** Writing – review & editing, Conceptualization; **Narcisa Burtea:** Writing – review & editing.

Data availability

The authors do not have permission to share data.

Declaration of competing interest

The authors declare that they have no known competing financial interests or personal relationships that could have appeared to influence the work reported in this paper.

References

[1] L. Bertsch, M. Pott-Polenske, F. Wienke, J. Kurz, J. Delfs, Retrofit measures for aircraft noise reduction: simulation benchmark and impact assessment, J. Aircr. 62 (2024) 191–206. https://doi.org/10.2514/1.C037819
[2] R. Zamponi, F. Avallone, D. Ragni, C. Schram, S. Van Der Zwaag, Relevance of quadrupolar sound diffraction on flow-induced noise from porous-coated cylinders, J. Sound Vib. 583 (2024) 118430. https://doi.org/10.1016/j.jsv.2024.118430
[3] C. Lyu, P. Liu, T. Hu, Q. Qu, X. Geng, T. Sun, H. Guo, R. Akkermans, Numerical investigations on phase cancelation of interaction noise for counter-rotating propellers, AIAA J. 62 (2024) 1826–1839. https://doi.org/10.2514/1.J063347
[4] E. Grande, S. Shubham, F. Avallone, D. Ragni, D. Casalino, Computational aeroacoustic study of co-rotating rotors in hover, Aerosp. Sci. Technol. 153 (2024) 109381. https://doi.org/10.1016/j.ast.2024.109381
[5] J. Goyal, T. Sinnige, F. Avallone, C. Ferreira, Benchmarking of aerodynamic models for isolated propellers operating at positive and negative thrust, AIAA J. 62 (2024) 3758–3775. https://doi.org/10.2514/1.J064093
[6] J. Goyal, F. Avallone, T. Sinnige, Isolated propeller aeroacoustics at positive and negative thrust, Aerosp. Sci. Technol. 147 (2024) 109021. https://doi.org/10.1016/j.ast.2024.109021
[7] D. Vittal Shenoy, R. Gojon, T. Jardin, M.C. Jacob, Aerodynamic and acoustic study of a small scale lightly loaded hovering rotor using large eddy simulation, Aerosp. Sci. Technol. 150 (2024) 109219. https://doi.org/10.1016/j.ast.2024.109219
[8] P. Li Volsi, G. Brogna, R. Gojon, T. Jardin, H. Parisot-Dupuis, J.M. Moschetta, Analysis of MAV rotors optimized for low noise and aerodynamic efficiency with operational constraints, Fluids 9 (2024) 96. https://doi.org/10.3390/fluids9040096
[9] B. Sarikaya, A. Zarri, J. Christophe, M.H. Aissa, T. Verstraete, C. Schram, Aerodynamic and aeroacoustic design optimization of UAVs using a surrogate model, J. Sound Vib. 589 (2024) 118539. https://doi.org/10.1016/j.jsv.2024.118539
[10] R. Wickersheim, M. Keßler, J. Sembowski, D. Bongen, P.J. Gomes, Numerical investigation and validation of noise sources of a distributed propulsion system, AIAA J. (2024) 1–13. https://doi.org/10.2514/1.J064531
[11] D. Granata, A. Savino, D. Grassi, L. Riccobene, A. Zanotti, Aerodynamic and aeroacoustics investigation of tandem propellers in hover for eVTOL configurations, Aerosp. Sci. Technol. 155 (2024) 109740. https://doi.org/10.1016/j.ast.2024.109740
[12] A. Zanotti, D. Granata, A. Savino, F. Caccia, L. Abergo, A. Guardone, J. Yin, R. Wickersheim, M. Kessler, A. Visingardi, M. Barbarino, A. Haas, H. Kaltenbach, G. Reboul, G. Bernardini, C. Poggi, Acoustic and aerodynamic evaluation of POLIMI tandem propellers configurations within GARTEUR AG26, in: 50th European Rotorcraft Forum, Marseille, France, 10–13 September, 2024.
[13] T. Bravo, C. Maury, D. Mazzoni, M. Amielh, Attenuation of low frequencies for ducted systems based on the acoustic black hole technique, in: Proceedings of ICSV 2024, International Congress on Sound and Vibration, Amsterdam, 2024.
[14] T. Bravo, C. Maury, Converging rainbow trapping silencers for broadband sound dissipation in a low-speed ducted flow, J. Sound Vib. 589 (2024) 118524. https://doi.org/10.1016/j.jsv.2024.118524
[15] D. Magliacano, G. Catapane, G. Petrone, K. Verdiere, O. Robin, Sound transmission properties of a porous metamaterial with periodically embedded Helmholtz resonators, Mech. Adv. Mater. Struct. 31 (25) (2023) 6748–6756. https://doi.org/10.1080/15376494.2023.2237699

[16] F. Kohlenberg, K. Knobloch, Experimental and numerical parameter study of a helmholtz resonator with a flexible wall, in: 30Th AIAA/CEAS Aeroacoustics Conference, 2024, American Institute of Aeronautics and Astronautics, 2024, pp. 1–15. https://doi.org/10.2514/6.2024-3077.
[17] J. Guzmán-Iñigo, A.S. Morgans, Designing the edges of holes (with bias flow) to maximise acoustic damping, J. Sound Vib. 575 (2024) 118224. https://doi.org/10.1016/j.jsv.2023.118224
[18] J. Guzmán-Iñigo, D. Ahmed, A.S. Morgans, Sensitivity and optimisation of the acoustic response of short circular holes with turbulent bias flow, J. Sound Vib. 618 (2025) 119322. https://doi.org/10.1016/j.jsv.2025.119322
[19] I. Moufid, R. Roncen, D. Matignon, E. Piot, Time-domain simulation of the acoustic nonlinear response of acoustic liners at high sound pressure level, Nonlinear Dyn. 112 (5) (2024) 3133–3162. https://doi.org/10.1007/s11071-023-09219-7
[20] S. Palleja-Cabre, I. Saraceno, P. Chaitanya, On the modification of tip leakage noise sources by over-tip liners, Phys. Fluids 36 (2) (2024) 026114. https://doi.org/10.1063/5.0187951
[21] M. Gennaretti, B. De Rubeis, C. Poggi, G. Bernardini, Deformable-boundary integral formulation for the solution of arbitrarily-forced acoustic wave equation, J. Sound Vib. 591 (2024) 118618. https://doi.org/10.1016/j.jsv.2024.118618
[22] O. Moriaux, R. Zamponi, C. Schram, Semi-empirical calibration of remote microphone probes using Bayesian inference, J. Sound Vib. 573 (2024) 118197. https://doi.org/10.1016/j.jsv.2023.118197
[23] O. Moriaux, Semi-Empirical Calibration using Bayesian inference (version 1.2), 2024, https://github.com/OMoriaux/SemiEmpiricalCalibrationBayesian.
[24] N. Hu, K.-S. Rossignol, Helmholtz resonance of pinhole-mounted sensors for wall pressure fluctuations measurements, in: AIAA Paper, 2024-3394, 2024. https://doi.org/10.2514/6.2024-3394
[25] C. Poggi, G. Bernardini, M. Gennaretti, A minimum objective function trim procedure for VTOLs noise reduction, Aerosp. Sci. Technol. 147 (2024) 109004. https://doi.org/10.1016/j.ast.2024.109004
[26] S. Schade, R. Jaron, L. Klähn, A. Moreau, Smart blade count selection to align modal propagation angle with stator stagger angle for low-noise ducted fan designs, Aerospace 11 (4) (2024). https://doi.org/10.3390/aerospace11040259
[27] S. Schade, R. Merino-Martinez, P. Ratei, S. Bartels, R. Jaron, A. Moreau, Initial study on the impact of speed fluctuations on the psychoacoustic characteristics of a distributed propulsion system with ducted fans, in: AIAA Scitech 2024 Forum, 2024. https://doi.org/10.2514/6.2024-3273
[28] A. Zarri, M.B. Botana, J. Christophe, C. Schram, Aerodynamic investigation of the turbulent flow past a louvered-fin-and-tube automotive heat exchanger, Exp. Therm. Fluid Sci. 155 (2024) 111182. https://doi.org/10.1016/j.expthermflusci.2024.111182
[29] G. Mazzeo, G. Petrone, S. De Rosa, F. Franco, I. Mohamed, O. Bareille, Experimental application of pseudo-equivalent deterministic excitation method through an impact test, J. Sound Vib. 579 (2024) 118372. https://doi.org/10.1016/j.jsv.2024.118372
[30] A. Piccolo, R. Zamponi, F. Avallone, D. Ragni, Turbulence distortion and leading-edge noise, Phys. Fluids 36 (12) (2024) 125183. https://doi.org/10.1063/5.0244627